

Type IIB Flux Vacua and Tadpole Cancellation

Philip Betzler and Erik Plauschinn*

We consider flux vacua for type IIB orientifold compactifications and study their interplay with the tadpole-cancellation condition. As a concrete example we focus on $T^6/\mathbb{Z}_2 \times \mathbb{Z}_2$, for which we find that solutions to the F-term equations at weak coupling, large complex structure and large volume require large flux contributions. Such contributions are however strongly disfavored by the tadpole-cancellation condition. We furthermore find that solutions which stabilize moduli in this perturbatively-controlled regime are only a very small fraction of all solutions, and that the space of solutions is not homogenous but shows characteristic void structures and vacua concentrated on submanifolds.

1. Introduction

String theory is argued to be a consistent theory of quantum gravity including gauge interactions. It is defined in ten space-time dimensions, and in order to make a connection to four-dimensional physics six spatial dimensions have to be compactified. Such compactifications have to satisfy a number of consistency conditions, for instance, in the presence of D-branes and closed-string fluxes the tadpole-cancellation condition and the Freed-Witten anomaly-cancellation condition have to be satisfied. (For a review of the former see [1] and for the latter see [2].) These conditions relate the closed- and open-string sectors to each other and put strong restrictions on the allowed background configurations. More concretely,

- 1) compactifications of string theory to four dimensions are typically performed on Calabi-Yau three-folds. The resulting effective theory contains a number of massless scalar fields corresponding to deformations of the background, which should be absent due to experimental constraints. A way to achieve this for type II theories is to deform the background geometry

by Neveu-Schwarz–Neveu-Schwarz (NS-NS) and Ramond-Ramond (R-R) fluxes, which generate a potential in the four-dimensional theory and provide mass-terms for the moduli fields. This procedure is called moduli stabilization, and for early work in the type IIB context see for instance^[3–5] and for work in the type IIA context see [6–8]. However, especially in the type IIB setting some of the moduli cannot be stabilized by (geometric) fluxes. One therefore includes non-perturbative effects which lead to the KKLT^[9] and large-volume^[10]

scenarios. Moduli stabilization often results in anti-de-Sitter or Minkowski vacua, while it is difficult to obtain de-Sitter solutions.^[11]

- 2) A gauge-theory sector for type II theories can be engineered using D-branes. D-branes filling four-dimensional space-time and wrapping submanifolds in the compact space have a gauge theory localized on their world-volume. Chiral matter can be localized at the intersection loci of different D-branes in the compact space, and in this way four-dimensional gauge theories can be constructed in a geometric way (for a review see for instance^[11]). However, when introducing D-branes one typically has to perform an orientifold projection of the theory. The fixed-loci of this projection correspond to orientifold planes which generically have negative mass and negative charge.


Moduli stabilization and the construction of a gauge-theory sector are two important aspects of connecting string theory to realistic four-dimensional physics. These tasks are often approached independently, however, as emphasized for instance in [12], there is a complicated interplay between them. This interplay can prevent moduli from being stabilized or can modify the stabilization procedure. Following this line of thought, the purpose of this paper is to study how parts 1) and 2) are connected via the tadpole-cancellation condition (schematically)

$$\text{fluxes} = \text{D-branes} + \text{O-planes}. \quad (1.1)$$

We approach this question by analyzing how properties of the space of flux vacua depends on the contribution of fluxes to the left-hand side of (1.1). We perform our analysis for the type IIB orientifold of $T^6/\mathbb{Z}_2 \times \mathbb{Z}_2$, and consider R-R three-form flux, geometric NS-NS H -flux as well as non-geometric NS-NS Q -flux. The geometric fluxes generically stabilize the complex-structure moduli and the axio-dilaton, while the non-geometric fluxes allow for stabilization of the Kähler moduli. We then determine distributions for how the values of the stabilized moduli depend

P. Betzler, E. Plauschinn
Arnold Sommerfeld Center for Theoretical Physics
Ludwig-Maximilians-Universität
Theresienstraße 37, 80333 München, Germany
E-mail: erik.plauschinn@lmu.de

P. Betzler
Max-Planck-Institut für Physik
Föhringer Ring 6, 80805 München, Germany

 The ORCID identification number(s) for the author(s) of this article can be found under <https://doi.org/10.1002/prop.201900065>

© 2019 The Authors. *Fortschritte der Physik* Published by Wiley-VCH Verlag GmbH & Co. KGaA. This is an open access article under the terms of the Creative Commons Attribution License, which permits use, distribution and reproduction in any medium, provided the original work is properly cited.

DOI: 10.1002/prop.201900065

on the tadpole contribution of the fluxes. Note that distributions of flux vacua have been discussed extensively in the literature before. For instance, for type IIB compactifications various aspects have been studied in [13–24] and for type IIA related work can be found in [8,25]. In the context of M-theory similar questions have been discussed in [26], and for F-theory see [27]. Recently also topological data analysis has been used to investigate properties of flux vacua in [28,29]. The main results of our analysis can be summarized as follows:

- We observe that the space of flux vacua is not homogenous but shows characteristic structures such as circular voids.^[16] We show furthermore that solutions can be accumulated on submanifolds in the space of solutions.
- We find that flux configurations which stabilize moduli in a weak-coupling, large complex-structure and/or large-volume regime are only a very small fraction of all possible configurations. The number of reliable flux vacua is therefore much smaller than naively expected.
- In order to stabilize moduli in a perturbatively-controlled regime at weak coupling, large complex structure and large volume, the flux contribution to the left-hand side of tadpole-cancellation condition (1.1) has to be larger than a certain threshold. The more reliable these vacua are required to be, the larger this threshold has to be. However, the contribution of D-branes and orientifold planes to the right-hand side of (1.1) is typically small. It is therefore difficult to perform moduli stabilization in a perturbatively-controlled regime and to satisfy the tadpole-cancellation condition.

Our findings for the structure of the space of flux vacua agree with for instance^[16,29] for the axio-dilaton, but we extend their analysis by including the complex-structure moduli. Our observation concerning the difficulty of obtaining reliable flux vacua is consistent with for instance^[30] who find that type IIB solutions at weak string-coupling are rare. Similarly, in [31] the authors argue that in order to avoid a certain runaway behaviour large fluxes have to be considered, also in [32] large fluxes are needed to obtain reliable solutions, and related difficulties are encountered in [33].

This work is organized as follows: in section 2 we review type IIB orientifold compactifications with geometric and non-geometric fluxes, we discuss the corresponding tadpole-cancellation conditions, we specialize to the example of the $\mathbb{T}^6/\mathbb{Z}_2 \times \mathbb{Z}_2$ orientifold and determine the relevant dualities. In section 3 we study moduli stabilization for the axio-dilaton, in section 4 we discuss the combined moduli stabilization of the axio-dilaton and the complex-structure moduli, and in section 5 we stabilize all of the closed-string moduli at tree-level. At the end of sections 3, 4 and 5 we have included brief summaries for each section, which may help the reader to get an overview of the main results. Our conclusions can be found in section 6.

2. Flux Compactifications

In this paper we are interested in compactifications of type IIB string theory on Calabi-Yau orientifolds with geometric and non-geometric fluxes. In order to fix our notation, we start in sections 2.1 and 2.2 by briefly reviewing orientifold compactifications and tadpole-cancellation conditions for general

Calabi-Yau three-folds. In section 2.3 we specialize to the example of $\mathbb{T}^6/\mathbb{Z}_2 \times \mathbb{Z}_2$, and in section 2.4 we discuss duality transformations for this background.

2.1. Orientifold Compactifications

Type IIB orientifold compactifications on Calabi-Yau three-folds give rise to a $\mathcal{N} = 1$ supergravity theory in four dimensions. This theory can be characterized in terms of a superpotential, Kähler potential and D-term potential, which we determine in the following.

Calabi-Yau Orientifolds

We begin with type IIB string theory on $\mathbb{R}^{3,1} \times \mathcal{X}$, where \mathcal{X} denotes a Calabi-Yau three-fold. The latter comes with a holomorphic three-form $\Omega \in H^{3,0}(\mathcal{X})$ and a real Kähler form $J \in H^{1,1}(\mathcal{X})$, and to perform an orientifold projection we impose a holomorphic involution σ on \mathcal{X} which acts on Ω and J as

$$\sigma^* J = +J \quad \sigma^* \Omega = -\Omega. \quad (2.1)$$

The involution leaves the non-compact four-dimensional part invariant, and hence the fixed loci of σ correspond to orientifold three- and seven planes. For the full orientifold projection σ is combined with $\Omega_p(-1)^{F_L}$, where Ω_p denotes the world-sheet parity operator and F_L is the left-moving fermion number. The latter two act on the bosonic fields in the following way

$$\begin{aligned} \Omega_p(-1)^{F_L} g &= +g, & \Omega_p(-1)^{F_L} B &= -B, \\ \Omega_p(-1)^{F_L} \phi &= +\phi, & \Omega_p(-1)^{F_L} C_{2p} &= (-1)^p C_{2p}, \end{aligned} \quad (2.2)$$

with g the metric, B the Kalb-Ramond field, ϕ the dilaton and C_{2p} the Ramond-Ramond potentials in type IIB. Since σ is an involution, the cohomology groups of the Calabi-Yau three-fold \mathcal{X} split into even and odd eigenspaces as $H^{p,q}(\mathcal{X}) = H_+^{p,q}(\mathcal{X}) \oplus H_-^{p,q}(\mathcal{X})$ ^[34] and for the discussion in this paper we assume that the corresponding Hodge numbers satisfy

$$h_+^{2,1} = 0, \quad h_-^{2,1} = 0. \quad (2.3)$$

However, more general cases can be considered as well. For the third de-Rham cohomology group $H^3(\mathcal{X})$ we choose a symplectic basis as follows

$$\{\alpha_I, \beta^J\} \quad \int_{\mathcal{X}} \alpha_I \wedge \beta^J = \delta_I^J, \quad I, J = 0, \dots, h_-^{2,1}, \quad (2.4)$$

with all other pairings vanishing. For the even Dolbeault cohomology groups we introduce bases

$$\begin{aligned} |g_{\mathcal{X}}|^{-1/2} d\text{vol}_{\mathcal{X}} &= \omega_0 \in H_+^{3,3}(\mathcal{X}), \\ \omega_A &\in H_+^{1,1}(\mathcal{X}), \\ \sigma^A &\in H_+^{2,2}(\mathcal{X}), \\ 1 &= \sigma^0 \in H_+^{0,0}(\mathcal{X}), \end{aligned} \quad A = 1, \dots, h_+^{1,1}, \quad (2.5)$$

where $|g_{\mathcal{X}}|$ denotes the determinant of the metric for \mathcal{X} . These bases can be chosen such that they satisfy a condition analogous to (2.4), in particular, we can require

$$\{\omega_A, \sigma^A\}, \quad \int_{\mathcal{X}} \omega_A \wedge \sigma^B = \delta_A^B, \quad A, B = 0, \dots, h_+^{1,1}. \quad (2.6)$$

Moduli

When compactifying string theory from ten to four dimensions, the deformations of the six-dimensional background become dynamical fields in the four-dimensional theory. These moduli fields are contained in the multiforms^[35]

$$\begin{aligned}\Phi^+ &= e^{-\phi} e^{B-iJ}, & \Phi_c^+ &= e^B C_{\text{mod}} + i \text{Re} \Phi^+, \\ \Phi^- &= \Omega, & &\end{aligned}\quad (2.7)$$

where the sum over all R-R potentials $C = \sum_p C_p$ has been separated into a flux contribution and a moduli contribution as $C = C_{\text{flux}} + C_{\text{mod}}$. Complex scalar fields τ and T_A can be determined by expanding Φ_c^+ into its zero- and four-form components as follows

$$\Phi_c^+ = \tau + T_A \sigma^A \equiv T_A \sigma^A, \quad (2.8)$$

where $T_0 \equiv \tau$ is called the axio-dilaton and T_A contain the Kähler moduli of \mathcal{X} . In general this expression also contains two-forms anti-invariant under σ , which are however vanishing due to our choice (2.3). The complex-structure moduli U^i with $i = 1, \dots, h_{-}^{2,1}$ are contained in the holomorphic three-form Ω .

Fluxes

We furthermore consider non-vanishing fluxes for the internal space. These are the R-R three-form flux $F = d C_{\text{flux}|3}$ as well as geometric and non-geometric fluxes in the NS-NS sector. The latter are the three-form flux H , the geometric flux f , and the non-geometric Q - and R -fluxes. These fluxes can be interpreted as operators acting on the differential forms as

$$\begin{aligned}H \wedge : p\text{-form} &\rightarrow (p+3)\text{-form}, \\ f \circ : p\text{-form} &\rightarrow (p+1)\text{-form}, \\ Q \bullet : p\text{-form} &\rightarrow (p-1)\text{-form}, \\ R \lrcorner : p\text{-form} &\rightarrow (p-3)\text{-form},\end{aligned}\quad (2.9)$$

and can be conveniently summarized using a generalized derivative operator^[36]

$$\mathcal{D} = d + H \wedge - f \circ + Q \bullet - R \lrcorner. \quad (2.10)$$

The precise action of the fluxes on the cohomology will be specified below. We furthermore summarize the action of the combined world-sheet parity and left-moving fermion number on the fluxes as follows^[36,37]

$$\begin{aligned}\Omega_p(-1)^{F_L} H &= -H, \\ \Omega_p(-1)^{F_L} f &= +f, & \Omega_p(-1)^{F_L} F &= -F \\ \Omega_p(-1)^{F_L} Q &= -Q, \\ \Omega_p(-1)^{F_L} R &= +R.\end{aligned}\quad (2.11)$$

For our assumption (2.3) this implies that f and R are vanishing. We also note that the R-R and NS-NS three-form fluxes have to satisfy quantization conditions of the form (see e.g. [38])

$$\int_{\Gamma} F \in \mathbb{Z}, \quad \int_{\Gamma} H \in \mathbb{Z}, \quad (2.12)$$

where $\Gamma \in H_3(\mathcal{X}, \mathbb{Z})$ is an arbitrary three-cycle on the Calabi-Yau three-fold \mathcal{X} . For orbifolds and orientifolds this condition can be modified, and we come back to this point on page 16 below. Furthermore, as will be explained in section 2.4, the NS-NS fluxes are related among each other through T-duality transformations, and hence also the geometric f - and the non-geometric Q - and R -fluxes should be appropriately quantized.

Supergravity Data

When compactifying type IIB string theory on orientifolds of Calabi-Yau three-folds, the resulting four-dimensional effective theory can be described in terms of $\mathcal{N} = 1$ supergravity.^[34] In particular, the Kähler potential takes the following form

$$\mathcal{K} = -\log[-i(\tau - \bar{\tau})] - 2 \log \hat{V} - \log \left[-i \int_{\mathcal{X}} \Omega \wedge \bar{\Omega} \right], \quad (2.13)$$

where \hat{V} denotes the volume of the Calabi-Yau manifold in Einstein frame. The superpotential is generated by the fluxes and can be expressed using the Mukai pairing $\langle \cdot, \cdot \rangle$ of the multiforms (2.7) and the generalized derivative (2.10) in the following way^[23,36,39]

$$\begin{aligned}W &= \int_{\mathcal{X}} \langle \Phi^-, F - \mathcal{D} \Phi_c^+ \rangle \\ &= \int_{\mathcal{X}} \Omega \wedge [F - \tau H - (Q \bullet \sigma^A) T_A].\end{aligned}\quad (2.14)$$

In general, the fluxes (2.9) also generate a D-term potential which can be expressed using the three-form part of $\mathcal{D}(\text{Im } \Phi^+)$ ^[37] (see also [40]). However, due to (2.11) the latter belongs to the σ -even third cohomology and vanishes when taking into account our requirements (2.3). In our setting therefore no D-term potential is generated.

Bianchi Identities and Tadpole-Cancellation Conditions

Finally, the R-R and NS-NS fluxes have to satisfy a number of Bianchi identities. These can be expressed using the generalized derivative \mathcal{D} as follows

$$\mathcal{D}^2 = \text{NS-NS sources}, \quad \mathcal{D}F = \text{R-R sources}, \quad (2.15)$$

where NS-NS sources stand for NS5-branes, Kaluza-Klein monopoles or non-geometric S_2 -branes (see for instance^[41] for a review and collection of references). However, in this work we assume these to be absent and therefore require $\mathcal{D}^2 = 0$. The R-R sources stand for orientifold planes and D-branes, and the second condition in (2.15) is also known as the tadpole cancellation condition. We discuss this condition in more detail in the following section.

2.2. Tadpole-Cancellation Condition

The tadpole-cancellation condition is an important consistency conditions for type I string theories. It links the closed-string to the open-string sector and puts strong constraints on the allowed D-brane configurations (for a review see for instance^[1]). From a conformal-field-theory point of view the tadpole-cancellation condition ensures the absence of UV divergencies in one-loop amplitudes (see e.g. [42,43] for textbook reviews) and therefore plays an important role for string theory being a consistent theory of gravity. From an effective-field-theory point of view, the tadpole-cancellation condition is the integrated version of the equation of motion for the R-R potentials and ensures the absence of certain anomalies in type II orientifold compactifications via the generalized Green-Schwarz mechanism.^[44] The tadpole-cancellation condition is thus an important consistency condition for string compactifications.

Explicit Expressions

We now formulate the tadpole-cancellation condition for the setting of the previous section. The contribution of the R-R-sources can be described using the charges^[45,46]

$$\begin{aligned} Q_{Dp} &= \text{ch}(\mathcal{F}) \wedge \sqrt{\frac{\hat{A}(\mathcal{R}_T)}{\hat{A}(\mathcal{R}_N)}} \wedge [\Gamma_{Dp}], \\ Q_{Op} &= Q_p \sqrt{\frac{\mathcal{L}(\mathcal{R}_T/4)}{\mathcal{L}(\mathcal{R}_N/4)}} \wedge [\Gamma_{Op}], \end{aligned} \quad (2.16)$$

where $[\Gamma_{Dp}]$ and $[\Gamma_{Op}]$ denote the Poincaré duals of the cycles wrapped by D-branes and O-planes in $\mathbb{R}^{1,3} \times \mathcal{X}$. The open-string gauge flux on the D-branes \mathcal{F} appears in the Chern character, the tangential and normal part of the curvature two-form \mathcal{R} appear in the \hat{A} -genus and the Hirzebruch polynomial \mathcal{L} , and $Q_p = -2^{p-4}$ denotes the charge of an orientifold p -plane. For more details we refer for instance to section 8.6 in [41]. Denoting the orientifold image of a Dp -brane with a prime, the Bianchi identity for the R-R fluxes then reads

$$dF = \sum_{Dp+Dp'} Q_{Dp} + \sum_{Op} Q_{Op}, \quad (2.17)$$

where the sum is over all D-branes and orientifold planes present in the background. The Freed-Witten anomaly-cancellation condition^[2] for D-branes takes the general form^[41,47]

$$DQ_{Dp} = 0, \quad DQ_{Op} = 0, \quad (2.18)$$

where we included the corresponding expression for an orientifold p -plane. Equation (2.17) can therefore be interpreted as a relation in D -cohomology.

For the setting discussed in this paper, the orientifold projection satisfies (2.1) and therefore leads to spacetime filling O3- and O7-planes. Taking into account (2.3) and that F in (2.17) is a

three-form flux, we find the following explicit expressions

$$\begin{aligned} Q \bullet F &= -2 \sum_{D7a} N_{D7a} [\Gamma_{D7a}] + 8 \sum_{O7b} [\Gamma_{O7b}], \\ H \wedge F &= -2 \left(N_{D3} - \frac{N_{O3}}{4} \right) \omega_0 \\ &\quad - \sum_{D7a} \text{tr}(\mathcal{F}_a)^2 \wedge [\Gamma_{D7a}] \\ &\quad + 2 \left(\sum_{D7a} N_{D7a} \frac{\chi(\Gamma_{D7a})}{24} + \sum_{O7b} \frac{\chi(\Gamma_{O7b})}{12} \right) \omega_0. \end{aligned} \quad (2.19)$$

Here, N_{D3} and N_{O3} denote the number of D3-branes and O3-planes, N_{D7a} denotes the number of coincident D7-branes in a stack a , $[\Gamma_{D7a}] = n_a^\Lambda \omega_\Lambda$ is the Poincaré dual of the cycle Γ_{D7a} expanded in the basis (2.5), \mathcal{F}_a is the (quantized) two-form gauge flux on the stack of D7-branes a in the fundamental representation, and $\chi(\Gamma)$ denotes the Euler number of the cycle Γ . The D-brane sums are over all D7-branes, and due to $h^{1,1} = 0$ the orientifold images give a factor of two. For details on the derivation of these expressions see for instance.^[48]

Orientifold Contributions

Let us now discuss the contribution of orientifold planes to the right-hand sides in (2.19). Typically orientifold planes give a positive contribution while D-branes give a negative contribution. For some classes of models the orientifold-contributions can be estimated as follows:

- For orientifolds of $\mathbb{T}^6/\mathbb{Z}_M$ or $\mathbb{T}^6/\mathbb{Z}_M \times \mathbb{Z}_N$ the numbers of O3- and O7-planes have been computed for instance in [49] for some examples. Here, the authors find that $N_{O3}, N_{O7} \lesssim 60$ and the contribution of the Euler numbers to (2.19) are vanishing. The contribution of orientifold planes to the right-hand sides of (2.19) is therefore typically positive and of order $\mathcal{O}(10)$.
- For del-Pezzo surfaces the possible orientifold projections have been classified in [50]. The number of orientifold three- and seven-planes are of order $\mathcal{O}(10)$, and in some examples the Euler numbers of the four-cycles are of order $\mathcal{O}(100)$. Also here, the contribution of orientifold planes to the right-hand side of (2.19) is positive and of order $\mathcal{O}(10)$.
- In F-theory the geometry of Calabi-Yau four-folds \mathcal{Y} encodes the geometry of D7-branes and orientifold planes in Calabi-Yau three-folds \mathcal{X} . If a lift from type IIB orientifolds to F-theory is possible, one finds that

$$\frac{\chi(\mathcal{Y})}{24} = \frac{N_{O3}}{4} + \sum_{D7a} N_{D7a} \frac{\chi(\Gamma_{D7a})}{24} + \sum_{O7b} \frac{\chi(\Gamma_{O7b})}{12}, \quad (2.20)$$

where $\chi(\mathcal{Y})$ denotes the Euler number of the Calabi-Yau four-fold \mathcal{Y} . In [51,52] a manifold \mathcal{Y}_{max} was identified with the largest known Euler number for a Calabi-Yau four-fold

$$\chi(\mathcal{Y}_{\text{max}}) = 1820448, \quad (2.21)$$

and more details for the present context can be found in [53]. Hence, for this example the contribution to the D3-tadpole in (2.19) is of order $\mathcal{O}(10^5)$.

D-Brane Contributions

We furthermore note that the tadpole-cancellation conditions (2.19) are the integrated versions of the R-R Bianchi identities (2.15). The former are therefore less restrictive than the latter, but for a proper string-theory solution also the Bianchi identities with localized sources have to be solved. When placing D-branes directly on top of orientifold planes solutions may be constructed more easily, but in general this is a difficult task (see for instance^[54]).

However, we can make the following general argument: because D-branes have a non-vanishing mass, their probe approximation breaks down when too many D-branes are placed into a compact space (away from the orientifold planes). In this case the back-reaction of D-branes on the geometry has to be taken into account, and an extreme case for this mechanism is the formation of black holes. It would be desirable to make this more precise, but we can argue that for ignoring back-reaction effects the contribution of D-branes to the right-hand sides in (2.19) should not be arbitrarily large.

Flux Contributions

Turning now to the flux contribution on the left-hand sides in (2.19), we note that for vanishing Q -flux the $H \wedge F$ -term typically has to be positive in order to obtain physically-relevant solutions. Since the right-hand sides are bounded from above by the orientifold contributions, the flux contributions should not be larger than $\mathcal{O}(10)$ to $\mathcal{O}(10^5)$. In the presence of non-geometric Q -flux the left-hand sides in (2.19) can be negative – but since also the D-brane contributions are bounded, again the flux contributions should not be too large. This is an important point for our approach in this paper, which we summarize as

In order to solve the tadpole-cancellation condition (2.19) and ignore the back-reaction of D-branes, the contribution of fluxes to the left-hand sides in (2.19) should not be too large. Depending on the setting, known bounds are of orders $\mathcal{O}(10)$ to $\mathcal{O}(10^5)$.

2.3. $\mathbb{T}^6/\mathbb{Z}_2 \times \mathbb{Z}_2$ Orientifold

Let us now turn to a specific example for a compactification space. We consider the orbifold $\mathbb{T}^6/\mathbb{Z}_2 \times \mathbb{Z}_2$ which provides a simple example of a Calabi-Yau three-fold with only few moduli. For our purposes it is sufficient to stay in the orbifold limit and not blow-up the fixed-point singularities, that is we ignore the twisted sectors. This model has been extensively studied in the literature, and we refer for instance to [55–58] for more details in the present context.

For this model the contribution of orientifold planes to the tadpole-cancellation condition (2.19) only allows for a small num-

ber of different flux choices. In order to be able to study general properties of the space of solutions, in the following we therefore ignore the precise form of the tadpole cancellation condition and allow for arbitrarily-large values of $H \wedge F$ and $Q \bullet F$. We do however keep in mind that these tadpole contributions are bounded by the D-brane and orientifold contributions.

Compactification Space

We start from the following six-dimensional orbifold construction which has the properties of a Calabi-Yau three-fold

$$\mathcal{X} = \frac{\mathbb{T}^2 \times \mathbb{T}^2 \times \mathbb{T}^2}{\mathbb{Z}_2 \times \mathbb{Z}_2}. \quad (2.22)$$

On each of the two-tori we introduce complex coordinates as

$$z^i = x^i + U^i y^i, \quad i = 1, 2, 3, \quad (2.23)$$

where x^i and y^i denote real coordinates with identifications $x^i \sim x^i + 1$ and $y^i \sim y^i + 1$, U^i denote the complex structures on each of the \mathbb{T}^2 , and no summation is performed in (2.23). The orbifold action is given by

$$\Theta : \begin{pmatrix} z_1 \\ z_2 \\ z_3 \end{pmatrix} \rightarrow \begin{pmatrix} -z_1 \\ -z_2 \\ +z_3 \end{pmatrix}, \quad \Theta' : \begin{pmatrix} z_1 \\ z_2 \\ z_3 \end{pmatrix} \rightarrow \begin{pmatrix} +z_1 \\ -z_2 \\ -z_3 \end{pmatrix}, \quad (2.24)$$

where Θ and Θ' are the two generators of the orbifold group $\mathbb{Z}_2 \times \mathbb{Z}_2$. In addition, we perform the following orientifold projection

$$\sigma : \begin{pmatrix} z_1 \\ z_2 \\ z_3 \end{pmatrix} \rightarrow \begin{pmatrix} -z_1 \\ -z_2 \\ -z_3 \end{pmatrix}. \quad (2.25)$$

Cohomology

Next, we turn to the cohomology of (2.22). We note that there are no one- or five-forms invariant under the orbifold action (2.24), and that the invariant three-forms are given by the following combinations

$$\begin{aligned} \alpha_0 &= dx^1 \wedge dx^2 \wedge dx^3, & \beta^0 &= +dy^1 \wedge dy^2 \wedge dy^3, \\ \alpha_1 &= dy^1 \wedge dx^2 \wedge dx^3, & \beta^1 &= -dx^1 \wedge dy^2 \wedge dy^3, \\ \alpha_2 &= dx^1 \wedge dy^2 \wedge dx^3, & \beta^2 &= -dy^1 \wedge dx^2 \wedge dy^3, \\ \alpha_3 &= dx^1 \wedge dx^2 \wedge dy^3, & \beta^3 &= -dy^1 \wedge dy^2 \wedge dx^3. \end{aligned} \quad (2.26)$$

Choosing the orientation of the six-dimensional space (2.22) such that we have $\int dx^1 \wedge dx^2 \wedge dx^3 \wedge dy^1 \wedge dy^2 \wedge dy^3 = 1$, the three-forms in (2.26) satisfy the intersection relation (2.4). We can furthermore define a holomorphic three-form

$$\Omega = dz^1 \wedge dz^2 \wedge dz^3, \quad (2.27)$$

which – when expanded in the basis (2.26) – takes the form¹

$$\Omega = \alpha_0 + (U^1 \alpha_1 + U^2 \alpha_2 + U^3 \alpha_3) - (U^2 U^3 \beta^1 + U^3 U^1 \beta^2 + U^1 U^2 \beta^3) + U^1 U^2 U^3 \beta^0. \quad (2.28)$$

Turning to the orientifold action (2.25), we see that all three-forms (2.26) are odd under σ and therefore $h_-^{2,1} = 3$ and $h_+^{2,1} = 0$. We also note that Ω is odd under the orientifold action as required by (2.1).

For the even cohomology we observe that the zero- and six-form cohomologies are even under the orbifold action (2.24). For the second cohomology we find the following invariant (1,1)-forms

$$\omega_A = \frac{i}{2 \operatorname{Im} U^A} dz^A \wedge d\bar{z}^A, \quad A = 1, 2, 3, \quad (2.29)$$

with no summation over A , and we define invariant (2,2)-forms as

$$\sigma^1 = -\omega_2 \wedge \omega_3, \quad \sigma^2 = -\omega_3 \wedge \omega_1, \quad \sigma^3 = -\omega_1 \wedge \omega_2. \quad (2.30)$$

Note that these satisfy the relations shown in (2.6). For the orbifold (2.22) we can now define a real Kähler form in the following way

$$J = t^1 \omega_1 + t^2 \omega_2 + t^3 \omega_3, \quad (2.31)$$

where the t^A are the (real) Kähler moduli. The forms (2.29) and (2.30) are all even under the orientifold projection (2.25) and therefore $h_+^{1,1} = 3$ and $h_-^{1,1} = 0$. We also note that J is even under σ , in agreement with (2.1).

Moduli

With the explicit expressions for the even cohomologies discussed above, we can now determine the moduli fields contained in Φ_c^+ via Equation (2.8). For the R-R zero- and four-form potentials (purely in the internal space) we use the following conventions

$$C_0 = c_0, \quad C_4|_{\text{internal}} = c_1 \sigma^1 + c_2 \sigma^2 + c_3 \sigma^3, \quad (2.32)$$

and evaluating (2.8) in the present situation leads to

$$T_0 = \tau = c_0 + i e^{-\phi}, \quad \begin{aligned} T_1 &= c_1 + i t^2 t^3, \\ T_2 &= c_2 + i t^3 t^1, \\ T_3 &= c_3 + i t^1 t^2, \end{aligned} \quad (2.33)$$

with the Einstein-frame Kähler moduli defined as $t^A = e^{-\phi/2} t^A$. We also note that the R-R two-form potential C_2 is odd under the combined world-sheet parity and left-moving fermion number (cf. (2.2)) and should therefore be expanded in the

σ -odd (1,1)-cohomology, which however vanishes. Finally, the complex-structure moduli U^i are contained in Ω as can be seen from (2.28).

Fluxes

Let us now turn to the fluxes. Using the basis of three-forms (2.26), the NS-NS and R-R three-form fluxes can be expanded in the following way

$$F = f^I \alpha_I + f_I \beta^I, \quad H = h^I \alpha_I + h_I \beta^I, \quad (2.34)$$

where $I = 0, \dots, 3$. The expansion coefficients f^I, f_I, h^I, h_I are quantized due to the flux quantization conditions for F and H shown in (2.12). For the remaining fluxes in the NS-NS sector we note that due to (2.3) and (2.11), the geometric f - and the non-geometric R -flux vanish. The Q -flux is in general non-vanishing, and we specify it by its action on the third and fourth cohomology as

$$\begin{aligned} Q \bullet \alpha_I &= -q_I^A \omega_A, & Q \bullet \sigma^A &= q^{IA} \alpha_I + q_I^A \beta^I. \\ Q \bullet \beta^I &= +q^{IA} \omega_A, \end{aligned} \quad (2.35)$$

Here we have again $A = 1, 2, 3$ and the flux quanta are integers. In order to shorten the notation for our subsequent discussion, we combine the H -flux with the Q -flux by defining

$$q_I^0 = h_I, \quad q^{I0} = h^I. \quad (2.36)$$

Let us briefly discuss a subtlety concerning the flux quantization condition (2.12). It was first pointed out in [59] that on orbifold (or orientifold) spaces besides bulk cycles inherited from the covering space, twisted cycles of shorter length can exist. This implies that the quantization condition of the fluxes shown above is slightly modified. For the present example of the type IIB $T^6/\mathbb{Z}_2 \times \mathbb{Z}_2$ orientifold this observation has been mentioned in [23,60] and has been analyzed in detail for instance in [61,62]. More concretely, for $\mathbb{Z}_2 \times \mathbb{Z}_2$ orbifold actions with and without discrete torsion (see [63]) one finds that fluxes on generic bulk cycles have to satisfy

$$\begin{aligned} \text{without discrete torsion} & \quad f^I, f_I, q^{IA}, q_I^A \in 8\mathbb{Z}, \\ \text{with discrete torsion} & \quad f^I, f_I, q^{IA}, q_I^A \in 4\mathbb{Z}. \end{aligned} \quad (2.37)$$

As mentioned at the beginning of this subsection, in this paper we ignore the twisted sector which effectively implies that we consider models without discrete torsion.^[61] Fluxes will therefore be quantized in multiples of eight. In the literature similar orientifolds have been studied,^[13,16,20,23,60] although with slightly different quantization conditions.

Bianchi Identities

Turning to the Bianchi identities (2.15), we recall from (2.5) that the collective basis for the even cohomology is denoted by ω_A and from (2.34) and (2.35) that the R-R and NS-NS flux quanta are given by f_I, f^I, q_I^A and q^{IA} . For the left-hand side

¹ The expression (2.28) is the classical result; in the quantum theory the coefficients of α_I and β^I (i.e. the periods) typically receive quantum corrections. However, in the large complex-structure limit $\operatorname{Im} U^i \gg 1$ these corrections can be ignored.

of the Bianchi identities we then introduce the following general notation

$$\begin{aligned} \mathcal{D}F &= Q^A \omega_A, & Q^A &= f_I q^{IA} - f^I q_I^A, \\ \mathcal{D}H &= Q^{0B} \omega_B, & Q^{AB} &= q_I^A q^{IB} - q^{IA} q_I^B, \\ \mathcal{D}(Q \bullet \sigma^A) &= Q^{AB} \omega_B, \end{aligned} \quad (2.38)$$

where $A, B = 0, \dots, 3$. Note that these expressions can be combined into an anti-symmetric five-by-five matrix of the form

$$Q = \begin{pmatrix} 0 & +Q^B \\ -Q^A & Q^{AB} \end{pmatrix}, \quad A, B = 0, 1, \dots, 3. \quad (2.39)$$

The right-hand side of the Bianchi identities (2.15) correspond to NS-NS and R-R sources, and schematically we have the relations

$$\begin{aligned} Q^0 &\longleftrightarrow \text{O3-planes/D3-branes}, \\ Q^A &\longleftrightarrow \text{O7-planes/D7-branes}, \\ Q^{0A} &\longleftrightarrow \text{NS5-branes}, \\ Q^{AB} &\longleftrightarrow \text{5}_2^2\text{-branes}, \end{aligned} \quad (2.40)$$

where in particular Q^A for $A = 0, \dots, 3$ are the contributions to the R-R tadpole cancellation conditions (2.19). As mentioned above, in this paper we do not consider NS5-branes or non-geometric 5_2^2 -branes which leads to the requirement $Q^{AB} = 0$ for $A, B = 0, \dots, 3$.

Supergravity Data

Let us finally determine the Kähler and superpotential for the $\mathbb{T}^6/\mathbb{Z}_2 \times \mathbb{Z}_2$ orientifold compactification. Evaluating (2.13) we find for the Kähler potential

$$\mathcal{K} = - \sum_{A=0}^3 \log[-i(T_A - \bar{T}_A)] - \sum_{i=1}^3 \log[-i(U^i - \bar{U}^i)], \quad (2.41)$$

up to an irrelevant constant term. Turning to the superpotential (2.14), the expansions of the fluxes in (2.34) and (2.35) give rise to

$$\begin{aligned} W &= f_0 - q_0^A T_A \\ &+ U^i (f_i - q_i^A T_A) \\ &+ \frac{1}{2} \sigma_{ijk} U^i U^j (f^k - q^{kA} T_A) \\ &- \frac{1}{6} \sigma_{ijk} U^i U^j U^k (f^0 - q^{0A} T_A), \end{aligned} \quad (2.42)$$

where a summation over $A = 0, \dots, 3$ and $i = 1, 2, 3$ is understood. For ease of notation we also defined the symmetric symbol σ_{ijk} which has the only non-vanishing components

$$\sigma_{123} = \sigma_{132} = \sigma_{231} = \sigma_{213} = \sigma_{312} = \sigma_{321} = +1. \quad (2.43)$$

The scalar F-term potential is determined in terms of the Kähler \mathcal{K} and superpotential W according to

$$V_F = e^{\mathcal{K}} \left[D_\alpha W \bar{G}^{\alpha\bar{\beta}} D_{\bar{\beta}} \bar{W} - 3 |W|^2 \right], \quad (2.44)$$

where ϕ^α collectively labels the complex scalar fields of the theory. The Kähler metric is computed from the Kähler potential as $G_{\alpha\bar{\beta}} = \partial_\alpha \partial_{\bar{\beta}} \mathcal{K}$, and the covariant derivative reads

$$D_\alpha W = \partial_\alpha W + (\partial_\alpha \mathcal{K}) W. \quad (2.45)$$

We also note that due to our assumption $h_+^{2,1} = 0$ shown in (2.3), no D-term potential is generated by the fluxes.

2.4. Dualities

We now want to discuss dualities for the orientifold of $\mathbb{T}^6/\mathbb{Z}_2 \times \mathbb{Z}_2$ introduced in the previous section. We are interested in transformations which leave the physical properties of a system invariant but which are not necessarily symmetries of the action. In particular, we note that an extremum of the F-term potential (2.44) is reached for vanishing F-terms

$$0 = \partial_\alpha W + (\partial_\alpha \mathcal{K}) W, \quad (2.46)$$

and in our subsequent analysis we are interested in duality transformations which map solutions of (2.46) to new solutions.

Overall Sign-Change

Let us start by noting that the F-term potential (2.44) as well as the F-term Equations (2.46) are invariant under changing the sign of all fluxes^[23]

$$(f_I, f^I, q_I^A, q^{IA}) \longrightarrow (-f_I, -f^I, -q_I^A, -q^{IA}). \quad (2.47)$$

This \mathbb{Z}_2 transformation maps $W \rightarrow -W$, which indeed leaves the scalar potential (2.44), the Equations (2.46) and the tadpole contributions (2.38) invariant.

$SL(2, \mathbb{Z})$ for Complex-Structure Moduli U^i

Next, we consider the group of large diffeomorphisms for each of the two-tori in (2.22).^[23] For a single \mathbb{T}^2 this group is $SL(2, \mathbb{Z})$, which is generated by T - and S -transformations of the form

$$T: U^i \rightarrow U^i + 1, \quad S: U^i \rightarrow -1/U^i, \quad (2.48)$$

with $i = 1, 2, 3$. In order for the F-term Equation (2.46) to stay invariant under T -transformations, the fluxes have to transform in the following way

$$\begin{aligned} g_0 &\rightarrow g_0 - b^i g_i + \frac{1}{2} \sigma_{ijk} b^i b^j g^k + \frac{1}{6} \sigma_{ijk} b^i b^j b^k, \\ g_i &\rightarrow g_i - \sigma_{ijk} b^j g^k - \frac{1}{2} \sigma_{ijk} b^j b^k g^0, \\ g^i &\rightarrow g^i + b^i g^0, \\ g^0 &\rightarrow g^0, \end{aligned} \quad (2.49)$$

where (g_I, g^I) stands collectively for (f_I, f^I) and (q_I^A, q^{IA}) , and σ_{ijk} was defined in (2.43). Under S -transformations of the complex structure moduli, the fluxes transform as follows

$$U^1 \rightarrow -1/U^1, \quad \begin{aligned} g_0 &\rightarrow -g_1, & g^0 &\rightarrow -g^1, \\ g_1 &\rightarrow +g_0, & g^1 &\rightarrow +g^0, \\ g_2 &\rightarrow -g^3, & g^2 &\rightarrow +g^3, \\ g_3 &\rightarrow -g^2, & g^3 &\rightarrow +g^2, \end{aligned} \quad (2.50)$$

and similarly for U^2 and U^3 . Note that for the fluxes this is not a \mathbb{Z}_2 but a \mathbb{Z}_4 action, which is however reduced to \mathbb{Z}_2 using (2.47). We also note that for a simultaneous S -transformation of all three complex-structure moduli, the transformation reads

$$U^i \rightarrow -1/U^i, \quad \begin{aligned} g_I &\rightarrow +g^I, \\ g^I &\rightarrow -g_I. \end{aligned} \quad (2.51)$$

Furthermore, all Bianchi identities and tadpole contributions Q^A and Q^{AB} are invariant under these transformations.

T-Duality

We now turn to T-duality transformations. It is well-known that performing an odd number of T-dualities for type IIB string theory results in the type IIA theory and vice versa, and applying two or six T-dualities to type IIB string theory with O3-/O7-planes results in type IIB with O5-/O9-planes. For T-duality to map the present setting of type IIB with O3-/O7-planes to itself, we therefore have to perform four collective T-duality transformations.

Let us now consider more closely the $\mathbb{T}^6/\mathbb{Z}_2 \times \mathbb{Z}_2$ orientifold with O3-/O7-planes. Using the Buscher rules,^[64,65] a collective T-duality transformation^[66] say along the first and second \mathbb{T}^2 results in the following transformation of the moduli

$$\text{T-duality along } z^1, z^2: \quad \begin{cases} \tau \rightarrow T_3, \\ T_1 \rightarrow T_2, & U^1 \rightarrow -1/U^1, \\ T_2 \rightarrow T_1, & U^2 \rightarrow -1/U^2, \\ T_3 \rightarrow \tau. \end{cases} \quad (2.52)$$

In (2.52) we have only shown how the moduli transform, but also the fluxes transform in a non-trivial way under T-duality. However, (2.52) contains an S -transform of the complex-structure moduli U^1 and U^2 . To better show the underlying structure, let us undo the U^i transformation in (2.52) using (2.50). We then obtain the transformation

$$\begin{aligned} \tau &\rightarrow T_3, & q_I^1 &\leftrightarrow q_I^2, \\ T_1 &\rightarrow T_2, & q_I^3 &\leftrightarrow h^I, \\ T_2 &\rightarrow T_1, & q^{I1} &\leftrightarrow q^{I2}, \\ T_3 &\rightarrow \tau, & q^{I3} &\leftrightarrow h^I, \end{aligned} \quad (2.53)$$

which by a slight abuse of notation we will refer to as T-duality in the following. Similar transformations are obtained for T-duality along the second & third and first & third two-torus.²

² We also mention that the transformation of the moduli under T-duality shown in (2.53) was to be expected: for type IIB orientifolds the R-R zero- and four-form potentials C_0 and C_4 are the real parts of τ

We furthermore observe that the F-term Equations (2.46) are invariant under a permutation of the Kähler moduli T_A and fluxes (q_I^A, q^{IA}) . This is just a re-labelling of indices and corresponds to the permutation group S_3 . Using now the T-duality action (2.53) together with the permutation of Kähler moduli, we see that S_3 is enhanced to S_4 acting on $T_A = (T_0, T_A)$ and fluxes (q_I^A, q^{IA}) . Indeed, for $S_A^B \in S_4$ the superpotential (2.42) is invariant under

$$T_A \rightarrow S_A^B T_B, \quad \begin{aligned} q_I^A &\rightarrow q_I^B (S^{-1})_B^A, \\ q^{IA} &\rightarrow q^{IB} (S^{-1})_B^A, \end{aligned} \quad (2.54)$$

and the flux contribution to the Bianchi identities shown in (2.38) transform as

$$Q \rightarrow S^{-T} Q S^{-1}, \quad S = \begin{pmatrix} 1 & 0 \\ 0 & S_A^B \end{pmatrix}. \quad (2.55)$$

We emphasize that four collective T-duality transformations for type II orientifold compactification are permutations of moduli and fluxes. They do not correspond to transformations which invert T_A .

S-Duality

We finally consider the $SL(2, \mathbb{Z})$ duality of type IIB string theory. For vanishing Q -flux its action on the axio-dilaton and the F - and H -flux takes the following form

$$\tau \rightarrow \frac{a\tau + b}{c\tau + d} \quad \begin{pmatrix} F \\ H \end{pmatrix} \rightarrow \begin{pmatrix} a & b \\ c & d \end{pmatrix} \begin{pmatrix} F \\ H \end{pmatrix}, \quad \begin{pmatrix} a & b \\ c & d \end{pmatrix} \in SL(2, \mathbb{Z}), \quad (2.56)$$

where $a, b, c, d \in \mathbb{Z}$. In particular, this transformation leaves the F-term Equations (2.46) invariant. However, for non-vanishing Q -flux only part of this duality survives.

- For constant shifts of the axio-dilaton and the Kähler moduli T_A , the Kähler potential (2.41) as well as the superpotential (2.42) are invariant under

$$T_A \rightarrow T_A + b_A, \quad \begin{aligned} f_I &\rightarrow f_I + q_I^A b_A, \\ f^I &\rightarrow f^I + q^{IA} b_A, \\ q_I^A &\rightarrow q_I^A, \\ q^{IA} &\rightarrow q^{IA}, \end{aligned} \quad (2.57)$$

where the parameter b_A has to be quantized as $b_A \in \mathbb{Z}$. This corresponds to a gauge transformation of the R-R zero- and four-form potentials.

- For an S -transformation $\tau \rightarrow -1/\tau$ in the presence of non-geometric fluxes, the F-term Equations (2.46) are in general not invariant. To restore the $SL(2, \mathbb{Z})$ duality the authors of [68]

and T_A , respectively. Under a single T-duality the R-R potentials transform as $C_p \rightarrow C_{p \pm 1}$,^[67] where the upper/lower sign is for a transformation transversal/longitudinal to C_p . For a collective T-duality along four directions we therefore map $C_0 \rightarrow C_4$ and some components of $C_4 \rightarrow C_0$. This agrees with (2.53).

introduced additional non-geometric P -fluxes as the counterpart of the Q -fluxes. In this paper we do not consider such P -fluxes, but refer for instance to^[47,69–75] for more details on this topic.

3. Moduli Stabilization I

As a first example for moduli stabilization on the $\mathbb{T}^6/\mathbb{Z}_2 \times \mathbb{Z}_2$ orientifold we consider a specific choice of fluxes which stabilizes the axio-dilaton τ , fixes the complex-structure moduli U^i to a symmetric point but leaves the Kähler moduli T_A unstabilized. This setting has been studied for instance in [13,16,20], and here we use it as a toy model for the more involved settings in the subsequent sections.

3.1. Setting

We start by specifying the superpotential (2.42). We consider a configuration with vanishing non-geometric fluxes (2.35),

$$q_I{}^A = 0, \quad q^{IA} = 0, \quad (3.1)$$

which implies that the Kähler moduli T_A do not appear in the potential and hence are not stabilized. The remaining R-R and NS-NS fluxes (2.34) are chosen as follows

$$\begin{aligned} f^0 &= 3\tilde{f}^0, & f_1 &= f_2 = f_3 = -\tilde{f}^0, & \tilde{f}^0 &\in 8\mathbb{Z}, \\ f_0 &= 3\tilde{f}_0, & f^1 &= f^2 = f^3 = +\tilde{f}_0, & \tilde{f}_0 &\in 8\mathbb{Z}, \\ h^0 &= 3\tilde{h}^0, & h_1 &= h_2 = h_3 = -\tilde{h}^0, & \tilde{h}^0 &\in 8\mathbb{Z}, \\ h_0 &= 3\tilde{h}_0, & h^1 &= h^2 = h^3 = +\tilde{h}_0, & \tilde{h}_0 &\in 8\mathbb{Z}, \end{aligned} \quad (3.2)$$

where \tilde{h}^0 and \tilde{h}_0 should not be zero simultaneously. Since the superpotential W is independent of the Kähler moduli the F-term Equations (2.46) take the simple form

$$\begin{aligned} 0 &= F_{T_A} = \partial_{T_A} \mathcal{K} W, & 0 &= W, \\ 0 &= F_{U^i} = \partial_{U^i} W + \partial_{U^i} \mathcal{K} W, & \Rightarrow & 0 = \partial_{U^i} W, \\ 0 &= F_\tau = \partial_\tau W + \partial_\tau \mathcal{K} W, & 0 &= \partial_\tau W. \end{aligned} \quad (3.3)$$

Ignoring unphysical values for U^i and τ with negative or vanishing imaginary part, we obtain the following solution to (3.3)

$$U^1 = U^2 = U^3 = i \quad \tau = \frac{\tilde{f}_0 - i\tilde{f}^0}{\tilde{h}_0 - i\tilde{h}^0}. \quad (3.4)$$

The fluxes in (3.2) are not arbitrary but are subject to the Bianchi identities (2.38). Since all non-geometric Q -fluxes vanish, the only nontrivial condition is the D3-tadpole contribution

$$Q^0 = 12(\tilde{f}_0\tilde{h}^0 - \tilde{f}^0\tilde{h}_0) > 0, \quad (3.5)$$

where the requirement of Q^0 being positive is related to having $\text{Im } \tau > 0$. Note that due to the quantization condition for the fluxes in (3.2), Q^0 is a multiple of 768.

3.2. Finite Number of Solutions for Fixed Q^0

Next, we briefly review the arguments of [16,20] showing that the number of physically-distinct solutions (3.4) is finite for finite Q^0 . We restrict the values of the axio-dilaton τ to the fundamental domain of the corresponding $SL(2, \mathbb{Z})$ duality (2.56)

$$\mathcal{F}_\tau = \left\{ -\frac{1}{2} \leq \tau_1 \leq 0, |\tau|^2 \geq 1 \cup 0 < \tau_1 < +\frac{1}{2}, |\tau|^2 > 1 \right\}. \quad (3.6)$$

For ease of notation we express the axio-dilaton in terms of its real and imaginary part as $\tau = \tau_1 + i\tau_2$, and for the solution (3.4) to the F-term equations we have

$$\tau = \frac{\tilde{h}_0\tilde{f}_0 + \tilde{h}^0\tilde{f}^0}{(\tilde{h}_0)^2 + (\tilde{h}^0)^2} + \frac{i}{12} \frac{Q^0}{(\tilde{h}_0)^2 + (\tilde{h}^0)^2}. \quad (3.7)$$

For a fixed positive value of Q^0 the imaginary part of τ is bounded from above as $\tau_2 \leq \frac{Q^0}{768}$, since \tilde{h}_0 and \tilde{h}^0 are integer multiples of eight which cannot be zero simultaneously. We now argue along the following lines:

- The tadpole contribution Q^0 is invariant under the $SL(2, \mathbb{Z})$ transformations (2.56). Using then a T -transformations acting on the axio-dilaton as $\tau \rightarrow \tau + b$ with $b \in \mathbb{Z}$, we can bring τ_1 into the region $-\frac{1}{2} \leq \tau_1 < +\frac{1}{2}$. This T -transformation is a duality transformation, and therefore we have the equivalence

$$\tilde{f}_0 \sim \tilde{f}_0 + b\tilde{h}_0, \quad \tilde{f}^0 \sim \tilde{f}^0 + b\tilde{h}^0. \quad (3.8)$$

Choosing without loss of generality $\tilde{h}_0 \neq 0$, for fixed \tilde{h}_0 there are only finitely-many inequivalent values for \tilde{f}_0 given by

$$\tilde{f}_0 = 0, \dots, \tilde{h}_0 - 1. \quad (3.9)$$

- Next, using an S -transformation $\tau \rightarrow -1/\tau$ (possibly together with additional T -transformations) we can bring τ into the fundamental domain \mathcal{F}_τ . In \mathcal{F}_τ a lower bound for the imaginary part τ_2 is obtained by considering $\tau_1 = -\frac{1}{2}$ for which $\tau_2 \geq \sqrt{3}/2$. Using (3.7) we then find

$$0 < (\tilde{h}_0)^2 + (\tilde{h}^0)^2 \leq \frac{Q^0}{6\sqrt{3}} \quad (3.10)$$

which leaves only finitely many possibilities for the integers \tilde{h}_0, \tilde{h}^0 . Together with (3.9), this implies also a finite number of choices for \tilde{f}_0 .

- The remaining flux \tilde{f}^0 is now determined via the tadpole contribution Q^0 shown in (3.5).

In summary, for a fixed positive value of the D3-tadpole contribution Q^0 , the F-term Equations (3.3) have only a finite number of physically-distinct solutions for τ .

3.3. Space of Solutions

In [16,20] it was shown that the solutions (3.4) mapped to the fundamental domain for τ are not distributed homogeneously. In

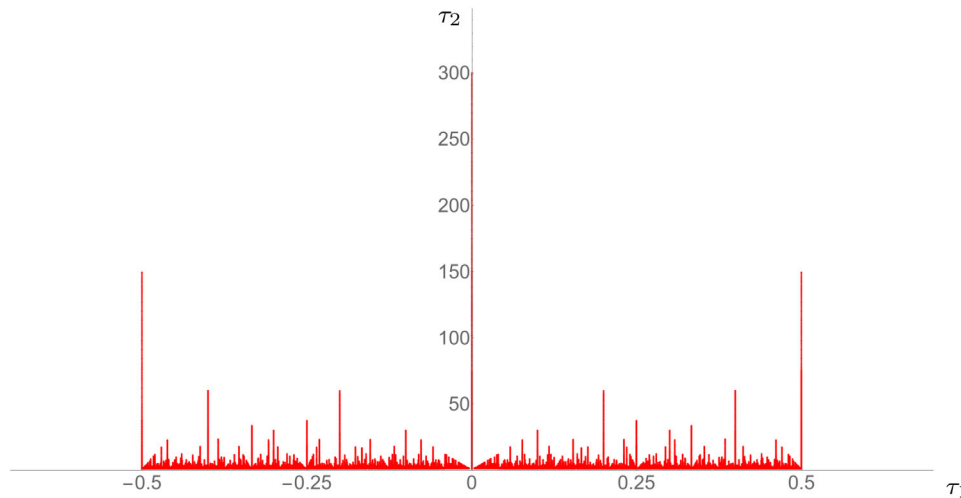


Figure 1. Space of solutions for the axio-dilaton τ with fluxes (3.2), mapped to the fundamental domain \mathcal{F}_τ . All solutions satisfy the bound $\frac{Q^0}{768} \leq \frac{Q_{\max}^0}{768} = 300$.

particular, the space of solutions contains voids with large degeneracies in their centers. In this section we review these findings and provide some new results on the dependence of these distributions on the D3-tadpole contribution Q^0 . Our data has been obtained using a computer algorithm to generate all physically-distinct flux vacua for a given upper bound on the D3-brane tadpole contribution.

Distribution of Solutions

As we argued above, for a fixed value of Q^0 , the number of physically inequivalent solutions for the axio-dilaton τ is finite. Using the $SL(2, \mathbb{Z})$ duality (2.56) we can map these solutions to the fundamental domain (3.6), and we have shown the corresponding space of solutions in **Figure 1** and **2**.

- For **Figure 1** we have included all flux configurations for which the tadpole contribution satisfies $0 < \frac{Q^0}{768} \leq 300$, and in order to have a symmetric plot we have added points on the boundary of the fundamental domain at $\tau_1 = \pm \frac{1}{2}$. We see that the space of solutions for (3.4) is bounded as $\tau_2 \leq 300$, and that solutions are located on lines with fixed τ_1 .
- In **Figure 2** we show a zoom of **Figure 1** for a small range of τ_2 . Here we see a characteristic structure of voids^[16] with accumulated points in their centers. The large voids are encircled by smaller ones, and we note that the higher density of points near $|\tau|^2 = 1$ is not a physical property as we have not taken into account the metric on moduli space.

Let us next note that the moduli space of the axio-dilaton τ is hyperbolic. Indeed from the Kähler potential (2.41) we can derive the corresponding Kähler metric with components

$$\mathcal{G}_{\tau_1 \tau_1} = \mathcal{G}_{\tau_2 \tau_2} = \frac{1}{4\tau_2^2}, \quad \mathcal{G}_{\tau_1 \tau_2} = 0. \quad (3.11)$$

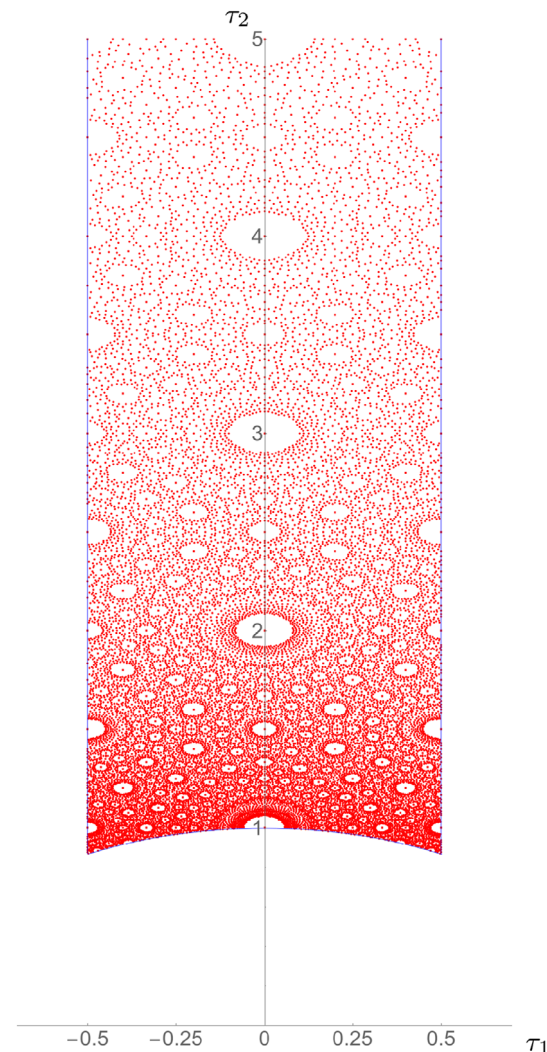


Figure 2. Zoom of **Figure 1** for a $0 \leq \tau_2 \leq 5$.

A convenient way to visualize this hyperbolic space is by mapping the Poincaré half-plane to the Poincaré disk via the conformal transformation

$$(\tau_1, \tau_2) \rightarrow (\tilde{\tau}_1, \tilde{\tau}_2) = \left(\frac{2\tau_1}{\tau_1^2 + (1+\tau_2)^2}, \frac{\tau_1^2 + \tau_2^2 - 1}{\tau_1^2 + (1+\tau_2)^2} \right). \quad (3.12)$$

The space of solutions for the axio-dilaton mapped to the Poincaré disk is then shown in **Figure 3**, which is the mapping of Figure 1 under (3.12).

- In Figure 3 the characteristic structure of voids is visible. In this plot effects of the moduli-space metric are incorporated.

Analysis of Voids

The number of physically-distinct solutions for the axio-dilaton is finite for fixed tadpole-contribution Q^0 . The number of solutions N with $Q^0 \leq Q_{\max}^0$ can be determined numerically, which leads to the following scaling behaviour

$$N \approx 0.823 \left[\frac{Q_{\max}^0}{768} \right]^2 \quad (3.13)$$

for large Q_{\max}^0 . We now want to study how the voids change depending on N , or, equivalently, depending on Q_{\max}^0 . In particular, we are interested how the size of the voids depends on Q_{\max}^0 . Qualitatively, this behaviour is illustrated in **Figure 4**:

- In Figure 4 the space of solutions for the axio-dilaton around the point $\tau = 2i$ is shown. The blue points correspond to solutions which satisfy $\frac{Q^0}{768} \leq 300$, and the red points correspond to solutions with $\frac{Q^0}{768} \leq 3000$. For larger Q_{\max}^0 the void around $\tau = 2i$ therefore becomes smaller, and finer void structures appear. These results are in agreement with the topological data analysis in [29].

Let us denote the origin of a void by τ_{void} , and define its size by the distance to the nearest solution τ_{sol} (not located at τ_{void}). The geodesic distance d is measured using the metric (3.11) on the axio-dilaton moduli space, for which we have

$$d(\tau, \tilde{\tau}) = \frac{1}{2} \operatorname{arccosh} \left[1 + \frac{(\tilde{\tau}_1 - \tau_1)^2 + (\tilde{\tau}_2 - \tau_2)^2}{2\tilde{\tau}_2\tau_2} \right]. \quad (3.14)$$

As we can see for instance from Figure 3, in the proper distance the voids can be approximated by a circle whose radius we define as

$$R_{\text{void}} = \min_{\tau_{\text{sol}} \neq \tau_{\text{void}}} d(\tau_{\text{void}}, \tau_{\text{sol}}). \quad (3.15)$$

The scaling behaviour of R_{void} with Q_{\max}^0 has been obtained for instance in [16,20] as $R_{\text{void}}^2 \sim 1/Q_{\max}^0$, and below we have determined the prefactors for some families of voids numerically. For voids located in the fundamental domain on the Poincaré plane we have the following relation between the radius of the void

R_{void} , the tadpole contribution Q_{\max}^0 and the number of solutions located at the center of the void n_{void}

$$\begin{aligned} R_{\text{void}}^2 &\approx \frac{1}{C \tau_{2\text{void}}} \left[\frac{768}{Q_{\max}^0} \right] & \begin{array}{c|c|c} \tau_{1\text{void}} & \tau_{2\text{void}} & C \\ \hline 0 & n & 4 \\ 0 & n+0.5 & 16 \\ \pm 0.2 & n+0.4 & 20 \\ \pm 0.2 & n+0.6 & 20 \end{array} \\ n_{\text{void}} &\approx \frac{2\pi}{C \tau_{2\text{void}}} \left[\frac{Q_{\max}^0}{768} \right] \end{aligned} \quad (3.16)$$

where $n \in \mathbb{Z}_+$. The constant C depends on the family of voids under consideration and can be read-off from the table in (3.16) for several examples. Note also that the number of solutions located at the center of the void divided by the area of the void takes the simple form

$$\frac{n_{\text{void}}}{2\pi R_{\text{void}}^2} \approx \left[\frac{Q_{\max}^0}{768} \right]^2. \quad (3.17)$$

Solutions at Small Coupling

The imaginary part of the axio-dilaton τ is bounded from above by the D3-tadpole contribution Q^0 , which via (2.33) implies a restriction on the string coupling g_s as

$$\tau_2 = e^{-\phi} = \frac{1}{g_s} \leq \frac{Q^0}{768} \Rightarrow g_s \geq \frac{768}{Q^0}. \quad (3.18)$$

Recall that in our conventions Q^0 is a multiple of 768. In the following we determine the number of physically-distinct solutions N_c which satisfy $\tau_2 \geq c$ for some cutoff $c > 0$ so that we have

$$\frac{768}{Q_{\max}^0} \leq g_s \leq \frac{1}{c}. \quad (3.19)$$

Note that in order to ignore string-loop corrections and corrections from world-sheet instantons, we need to stabilize the axio-dilaton at small g_s . This implies that Q^0 and c should be sufficiently large. Using then the exact data for the space of solutions, we can obtain fits for N_c for values of Q_{\max}^0 of the order $\frac{Q_{\max}^0}{768} = \mathcal{O}(10^3)$. In particular, with the scaling of the total number of solutions N shown in (3.13) we have

$$\begin{array}{c|c|c} c & N_c & N_c/N \\ \hline 2 & 0.393 \left[\frac{Q_{\max}^0}{768} \right]^2 & 0.478 \\ 5 & 0.157 \left[\frac{Q_{\max}^0}{768} \right]^2 & 0.191 \\ 10 & 0.078 \left[\frac{Q_{\max}^0}{768} \right]^2 & 0.095 \\ 20 & 0.039 \left[\frac{Q_{\max}^0}{768} \right]^2 & 0.047 \end{array} \quad \frac{Q_{\max}^0}{768} \gg 1 \quad (3.20)$$

We observe that in this limit the percentage of solutions with $g_s \ll 1$ is small and independent of Q_{\max}^0 . For instance, only about 5% of the solutions have a string coupling satisfying $g_s \leq 0.05$. However, the region of small tadpole contributions $\frac{Q^0}{768} = \mathcal{O}(1)$ is more interesting. Here the number of solutions N_c does not follow a simple quadratic behavior, and the precise numbers are shown in **Figure 5**. We see that for a particular c in

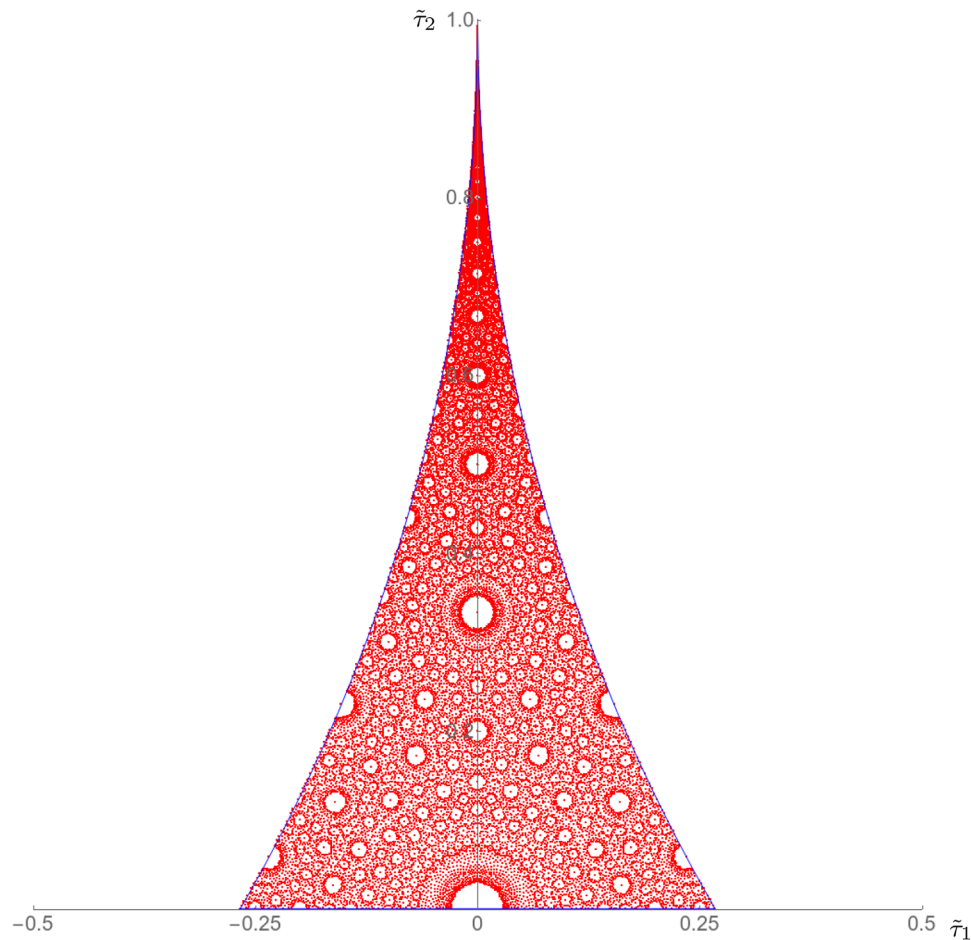


Figure 3. Space of solutions for the axio-dilaton τ with fluxes of the form (3.2), restricted to the fundamental domain and mapped to the Poincaré disk. All solutions satisfy the bound $\frac{Q^0}{768} \leq 300$.

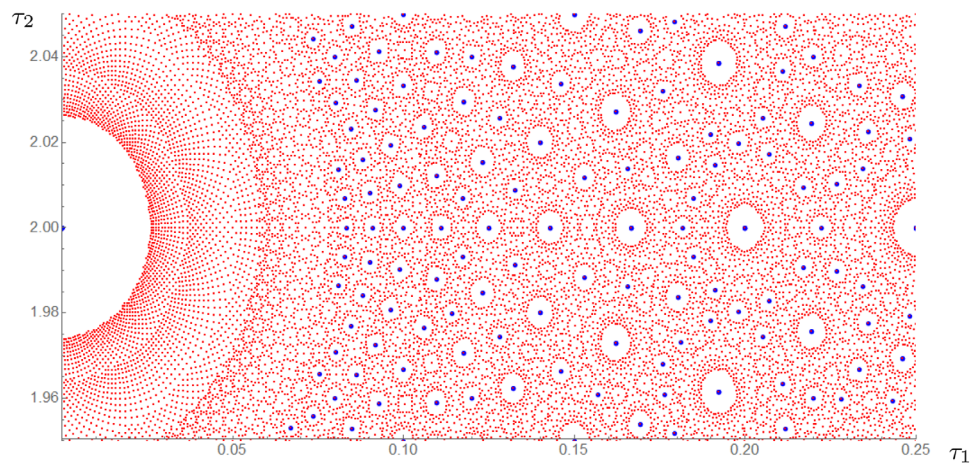


Figure 4. Space of solutions for the axio-dilaton τ with fluxes of the form (3.2) near $\tau = 2i$ on the Poincaré plane for $\frac{Q^0}{768} \leq 300$ (blue) and $\frac{Q^0}{768} \leq 3000$ (red).

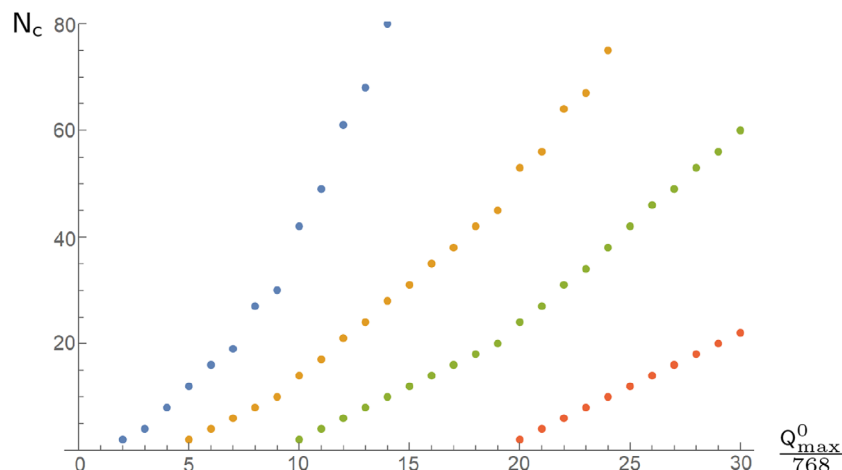


Figure 5. Number of solutions N_c (for the axio-dilaton τ with fluxes of the form (3.2)) which satisfy $c \leq \tau_2 \leq \frac{Q_{\max}^0}{768}$ for $c = 2, 5, 10, 20$ in colors blue, orange, green and red, respectively.

$g_s \leq 1/c$, the D3-tadpole contributions $\frac{Q^0}{768}$ has to be larger than some threshold. Furthermore, above this threshold the number of solutions is not large but only $\mathcal{O}(10)$.

3.4. Summary

Let us summarize the results and observations of this section for moduli stabilization of the axio-dilaton with the choice of fluxes given in Equation (3.4):

- As already known before, for a fixed D3-brane tadpole contribution Q^0 , the number of physically-distinct solutions to the F-term equations for the axio-dilaton τ is finite due to the corresponding $SL(2, \mathbb{Z})$ duality.^[16,20]
- The solutions for the axio-dilaton in the fundamental domain are not distributed homogeneously, but show characteristic void structures as illustrated in Figures 2 and 3.
- With increasing upper bound Q_{\max}^0 on the tadpole contribution, the area of these voids shrinks and the number of solutions located at the center n_{void} increases as shown in (3.16). The precise behaviour for the radius R_{void} and n_{void} is proportional to a constant depending on the location of the void, however, the ratio $n_{\text{void}}/2\pi R_{\text{void}}^2$ is universal.
- The string coupling is bounded from below by the tadpole contribution as $\frac{768}{Q^0} \leq g_s$. In order to ignore string corrections and trust the solutions (3.4), we have to demand $g_s \ll 1$ which implies $\frac{Q^0}{768} \gg 1$. This is in contrast to our discussion of the tadpole-cancellation condition on page 12 which requires $\frac{Q^0}{768}$ to be small, and illustrates the difficulty of obtaining reliable solutions to the F-term equations.
- We have furthermore analyzed the number of physically-distinct solutions satisfying $g_s \leq 1/c$. Requiring a small string coupling of for instance $g_s \leq 1/10$, we find that only about 10% of the solutions satisfy this condition. If we require g_s to be smaller, then the corresponding fraction of solutions is smaller.

4. Moduli Stabilization II

In this section we extend our previous discussion by including the complex-structure moduli U^i . We choose flux configurations which stabilize the axio-dilaton and fix the complex-structure moduli at an isotropic minimum with $U^1 = U^2 = U^3$. Such vacua have previously been studied for instance in [20,60].

4.1. Setting

We start again by specifying the superpotential (2.42) and set to zero the non-geometric fluxes (2.35)

$$q_I^A = 0, \quad q^{IA} = 0 \quad (4.1)$$

and for the R-R and remaining NS-NS fluxes (2.34) we choose the following restricted setting

$$\begin{aligned} f_1 = f_2 = f_3, \quad h_1 = h_2 = h_3, \\ f^I, f_I, h^I, h_I \in 8\mathbb{Z}. \end{aligned} \quad (4.2)$$

Since the superpotential is independent of the Kähler moduli T_A , the F-term Equations (2.46) simplify as in (3.3) and we obtain

$$0 = W, \quad 0 = \partial_{U^i} W, \quad 0 = \partial_{\tau} W. \quad (4.3)$$

Due to the isotropic choice of fluxes in (4.2), the complex-structure moduli U^i are stabilized such that

$$U^1 = U^2 = U^3 =: U, \quad (4.4)$$

and the F-term Equations (4.3) reduce to

$$\begin{aligned} -f_0 - 3U f_1 - 3(U)^2 f^1 + (U)^3 f^0 &= 0, \\ -h_0 - 3U h_1 - 3(U)^2 h^1 + (U)^3 h^0 &= 0, \end{aligned} \quad (4.5)$$

$$(f_1 - \tau h_1) + 2 U(f^1 - \tau h^1) - (U)^2(f^0 - \tau h^0) = 0. \quad (4.6)$$

The R-R and NS-NS fluxes in (4.2) are furthermore subject to the Bianchi identities (2.38), and due to the vanishing Q -fluxes the only nontrivial relation is again given by the D3-brane tadpole contribution

$$Q^0 = f_0 h^0 - f^0 h_0 + 3(f_1 h^1 - f^1 h_1) > 0. \quad (4.7)$$

Note that due to the quantization condition for the fluxes, the tadpole contribution Q^0 is an integer multiple of 64. However, as it has been explained in footnote 10 of [60], in order to obtain physically-viable solutions Q^0 receives an additional factor of three. The tadpole contribution is therefore always a multiple of 192, which is also what we see explicitly in our data.

4.2. Finite Number of Solutions for Fixed Q^0

The two equations for the complex-structure modulus shown in (4.5) define an overdetermined cubic system for U , which in general does not allow for a solution in closed form. Since the coefficients in (4.5) are real, one can bring these equations into the form

$$(U - u_0)(U - u_1)(U - \bar{u}_1) = 0, \quad u_0 \in \mathbb{R}, \quad u_1 \in \mathbb{C}, \quad (4.8)$$

where u_0, u_1, \bar{u}_1 denote the solutions. Physically-acceptable solutions have to satisfy $\text{Im } U > 0$, and therefore the F-term equations (4.5) have at most one solution for U of interest to us. The Equation (4.6) can be solved for the axio-dilaton as

$$\tau = \frac{f_1 + 2 U f^1 - (U)^2 f^0}{h_1 + 2 U h^1 - (U)^2 h^0}, \quad (4.9)$$

which however depends on U . More details on these solutions can be found in appendix A, where we follow the discussion of [20,60]. As reviewed in section 2.4, in the absence of non-geometric Q -fluxes the axio-dilaton and the complex-structure moduli enjoy $SL(2, \mathbb{Z})$ dualities. These can be used to bring τ and U into their fundamental domains

$$\mathcal{F}_\tau = \left\{ -\frac{1}{2} \leq \tau_1 \leq 0, |\tau|^2 \geq 1 \cup 0 < \tau_1 < +\frac{1}{2}, |\tau|^2 > 1 \right\},$$

$$\mathcal{F}_U = \left\{ -\frac{1}{2} \leq U_1 \leq 0, |U|^2 \geq 1 \cup 0 < U_1 < +\frac{1}{2}, |U|^2 > 1 \right\}, \quad (4.10)$$

where we again split τ and U into their real and imaginary parts as $\tau = \tau_1 + i \tau_2$ and $U = U_1 + i U_2$. We furthermore note that the two $SL(2, \mathbb{Z})$ dualities leave the D3-tadpole contribution Q^0 invariant. Now, as shown by [20,60] and reviewed in appendix A, the dualities can be used to show that the number of physically-distinct vacua in the fundamental domain is finite for fixed Q^0 . In the following we explore how the properties of the space of solutions for τ and U depend on Q^0 .

4.3. Space of Solutions

In this section we study the space of solutions to the F-term Equations (2.46) for the combined axio-dilaton and complex-structure-modulus system. Since for the axio-dilaton system we found two-dimensional circular voids in the two-dimensional moduli space, it is natural to expect four-dimensional spherical voids in the four-dimensional moduli space. However, we can not confirm this expectation. Our data has again been obtained using a computer algorithm, which generated all physically-distinct flux vacua for a given upper bound on the D3-brane tadpole contribution Q^0 .

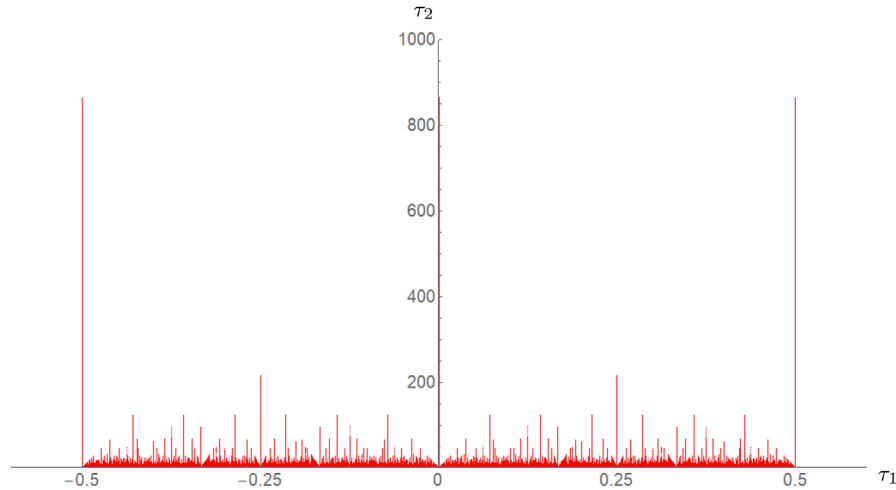
Distribution of Solutions

In [20,60] (as well as in appendix A) it is shown that for fixed Q^0 the number of physically-distinct solutions is finite. We have determined all solutions for the setting described in section 4.1 numerically, and have visualized them in the following figures.

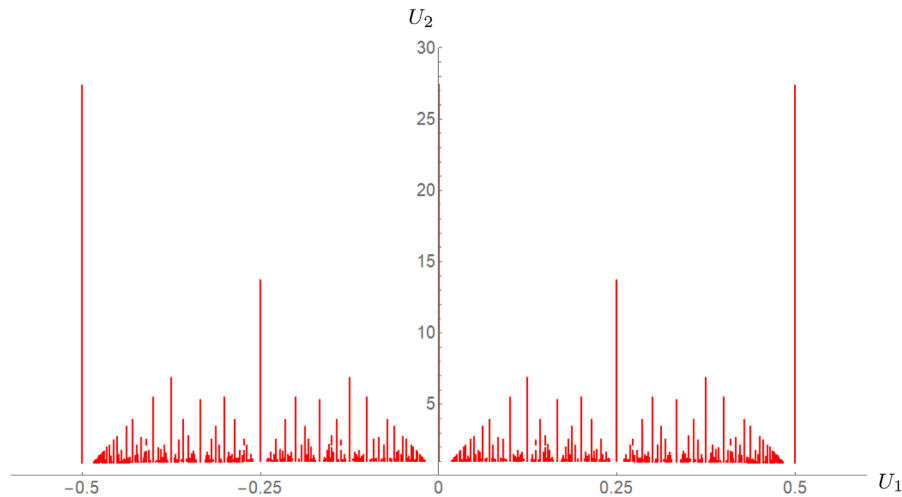
- In **Figure 6** we have shown the solutions for the fluxes of the form (4.2) projected onto the τ and onto the U -plane.^[20] All solutions satisfy the bound on the tadpole contribution $\frac{Q^0}{192} \leq 1000$, and in order to have a symmetric plot we included points on the boundary of the fundamental domains. These plots are similar to the one in Figure 1. When comparing Figures 6a and 6b, we note that for the same Q^0 the maximum values for τ_2 and U_2 differ significantly. Furthermore, we note that the number of different values for τ_1 is much larger than for U_1 .
- In **Figure 7** we show sections through the four-dimensional space of solutions for $\tau_2 \leq 2$, characterized by different values of the complex-structure modulus. All solutions satisfy $\frac{Q^0}{192} \leq 1000$, and these plots show void structures similar as in Figure 2. We note however that although the location of the voids stays the same when going from $U = i$ to $U = 2i$ and similarly from $U = \sqrt{2}i$ to $U = 2\sqrt{2}i$, the density of solutions decreases. This appears to be a general feature which we observe in the data.
- In **Figure 8** we have shown three-dimensional sections of the four-dimensional space of solutions for $U_1 = 0$. All solutions have been mapped to the fundamental domain. Figures 8a and 8b show two different points of view, which illustrate that the three-dimensional section of the space of solutions is not homogenous. Solutions are accumulated on planes for particular values of U_2 , while the space between these planes is only sparsely populated. This is in agreement with our observations in Figure 7, which also show that the density of solutions varies.

The lines in Figure 8a and 8b connect voids for different values of U_2 and are described by the following equations for $t \in \mathbb{R}_+$

$$\begin{aligned} \text{orange} \quad l_1 \quad (\tau_1, \tau_2, U_1, U_2) &= (0, 1+t, 0, 1+\frac{1}{1}t), \\ \text{red} \quad l_2 \quad (\tau_1, \tau_2, U_1, U_2) &= (0, 2+t, 0, 1+\frac{1}{2}t), \\ \text{purple} \quad l_3 \quad (\tau_1, \tau_2, U_1, U_2) &= (0, 3+t, 0, 1+\frac{1}{3}t), \\ \text{green} \quad l_4 \quad (\tau_1, \tau_2, U_1, U_2) &= (-\frac{1}{2}, \frac{3}{2}+t, 0, 1+\frac{2}{3}t). \end{aligned} \quad (4.11)$$



(a) Projection of solutions onto the τ -plane.



(b) Projection of solutions onto the U -plane.

Figure 6. Space of solutions for the setting described in section 4.1, mapped to the fundamental domains \mathcal{F}_τ and \mathcal{F}_U and projected onto the τ - and U -plane. All solutions satisfy the bound $\frac{Q^0}{192} \leq 1000$.

- In **Figure 9** we have shown the same three-dimensional section of the space of solutions as in **Figure 8**. The point of view in **Figure 9a** is along the line l_1 (orange) of (4.11) and the point of view in **Figure 9b** is along the line l_2 (red). In these three-dimensional sections of the four-dimensional space of solutions we therefore have a cylindrical void centered around the lines in (4.11).

Solutions at Small Coupling and Large Complex Structure

We now consider the number N of physically-distinct solutions for the combined axio-dilaton and complex-structure moduli system defined in section 4.1. This number is finite for fixed D3-tadpole contribution Q^0 , and since we have the numerical data

we can determine this number explicitly. For large Q^0 the dependence takes the form

$$N \approx 1.2501 \left[\frac{Q^0}{192} \right]^2. \quad (4.12)$$

We next note that in the fundamental domains, the imaginary parts of the axio-dilaton and complex-structure moduli satisfy a lower bound similarly as in the previous example. An upper bound can be obtained from the numerical data, which can be expressed as³

³ More precisely, with $x = \frac{Q^0}{192}$ the bound on U_2 can be expressed as $U_2 \leq \sqrt{C} x$, where the constant C takes values $C = 3/4$ for $x = 0, 1 \pmod{4}$, $C = 3/8$ for $x = 2 \pmod{8}$, $C = 1/4$ for $x = 3, 7 \pmod{8}$, and $C = 1/8$ for $x = 6 \pmod{8}$.

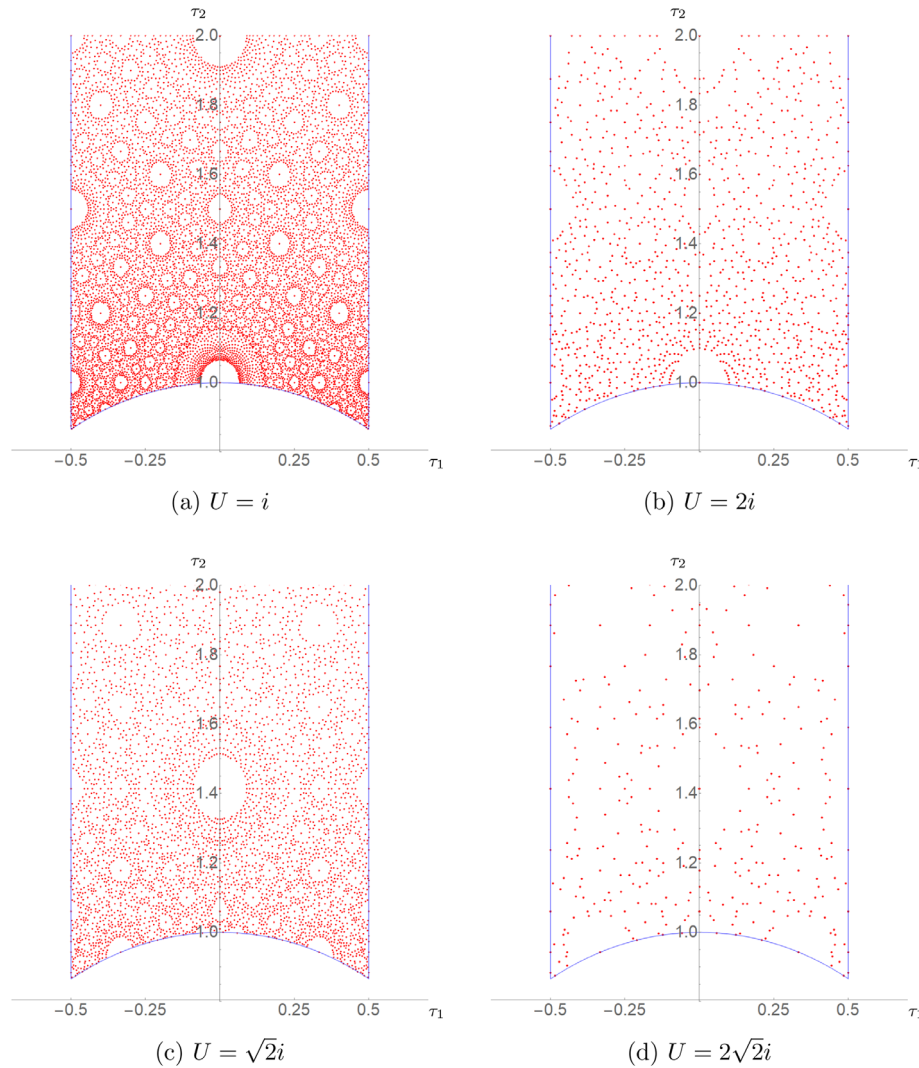


Figure 7. Section through the four-dimensional space of solutions for the setting described in section 4.1. The solutions have been mapped to the fundamental domains, and the sections are for fixed complex-structure modulus at $U = i$, $U = 2i$, $U = \sqrt{2}i$ and $U = 2\sqrt{2}i$. All solutions satisfy the bound $\frac{Q^0}{192} \leq 1000$.

$$\frac{\sqrt{3}}{2} \leq \tau_2 \leq \frac{\sqrt{3}}{2} \left[\frac{Q^0}{192} \right], \quad \frac{\sqrt{3}}{2} \leq U_2 \leq \frac{\sqrt{3}}{2} \left[\frac{Q^0}{192} \right]^{1/2}. \quad (4.13)$$

Note that in our conventions the tadpole contribution Q^0 is a multiple of 192. However, as we have seen in (4.9), the solution for the axio-dilaton depends on the complex-structure modulus. Although this dependence is difficult to analyze analytically, the numerical data gives the following bound on the solutions

$$\tau_2 U_2 \leq \frac{3}{4} \frac{Q^0}{192}. \quad (4.14)$$

This bound is stronger than in (4.13), and it implies that for fixed Q^0 the imaginary parts of τ and U cannot be made simultaneously large. In particular, in order to have solutions at small coupling $g_s = \frac{1}{\tau_2} \ll 1$ and large complex structure $U_2 \gg 1$, the tadpole contribution has to be sufficiently large. Let us make this

more precise and determine numerically the number of solutions N_c with $Q^0 \leq Q_{\max}^0$ for which

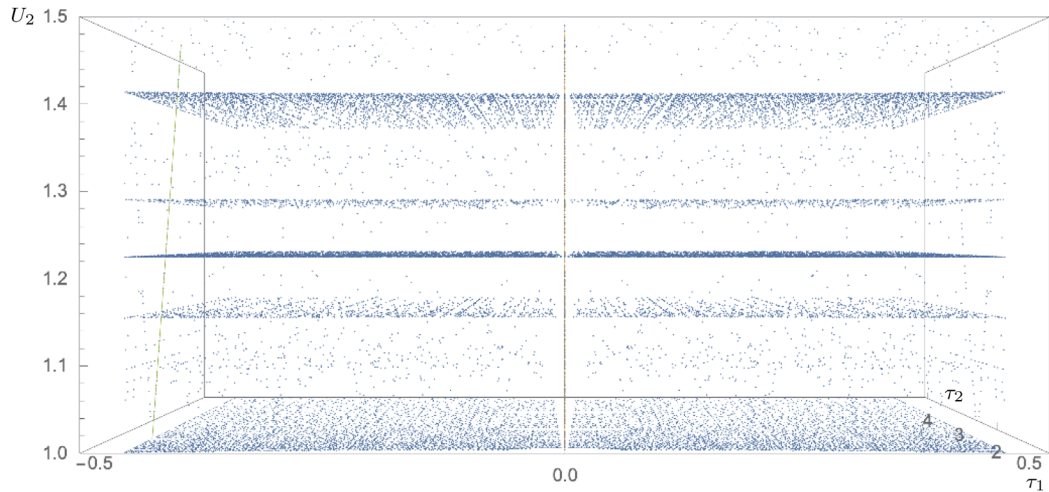
$$g_s \leq \frac{1}{c} \quad \text{and} \quad U_2 \geq c. \quad (4.15)$$

In the limit of large $\frac{Q_{\max}^0}{192}$ we obtained the following approximations

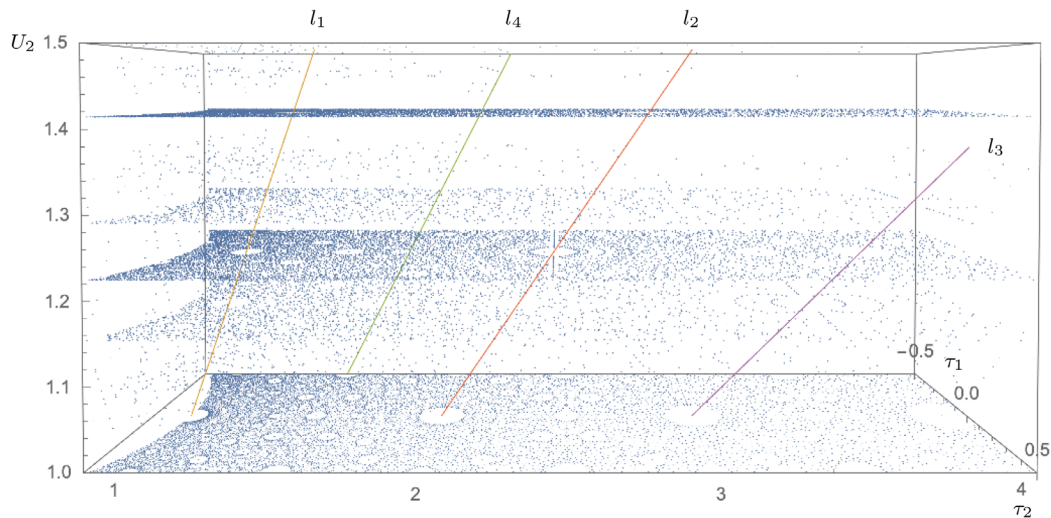
c	N_c	N_c/N
2	$0.0553 \left[\frac{Q_{\max}^0}{192} \right]^2 - 3.4617 \left[\frac{Q_{\max}^0}{192} \right]$	0.041
5	$0.0047 \left[\frac{Q_{\max}^0}{192} \right]^2 - 0.7627 \left[\frac{Q_{\max}^0}{192} \right]$	0.004
10	$0.0009 \left[\frac{Q_{\max}^0}{192} \right]^2 - 0.3569 \left[\frac{Q_{\max}^0}{192} \right]$	0.001

(4.16)

These approximations do not describe the data very well, but are sufficient for our purposes here. In particular, we see that at



(a) Point of view along the τ_2 -direction.



(b) Point of view along the τ_1 -direction.

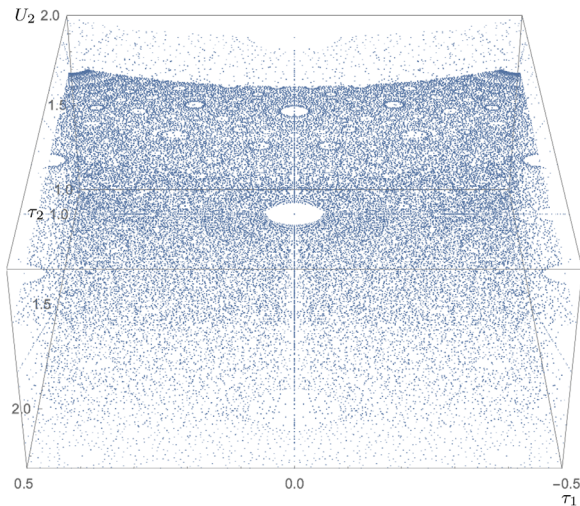
Figure 8. Section through the four-dimensional space of solutions with $U_1 = 0$ for the setting described in section 4.1. All solutions satisfy the bound $\frac{Q^0}{192} \leq 1000$ and have been mapped to the fundamental domains. The lines in 8a and 8b connect voids for different values of U_2 and are described by the expressions in Equation (4.11).

leading order N_c depends quadratically on Q_{\max}^0 and that the ratios N_c/N are rather small. Thus, only a small percentage of the solutions to the F-term equations are in a perturbatively-controlled regime. More interesting is the limit of small $\frac{Q^0}{192}$, which we have illustrated in **Figure 10**. We see that for $c = 2$ (blue) there are solutions starting at $\frac{Q^0}{192} = 16$. For $c = 5$ (orange) we find solutions starting at $\frac{Q^0}{192} = 100$, and for $c = 10$ (green) solutions can be obtained starting at $\frac{Q^0}{192} = 400$. The main conclusion we want to draw from this analysis is that for solutions at weak coupling $g_s \ll 1$ and large complex structure $U_2 \gg 1$, the D3-tadpole contribution $\frac{Q^0}{192}$ has to be large. As discussed on page 12, this is in tension with the tadpole cancellation condition.

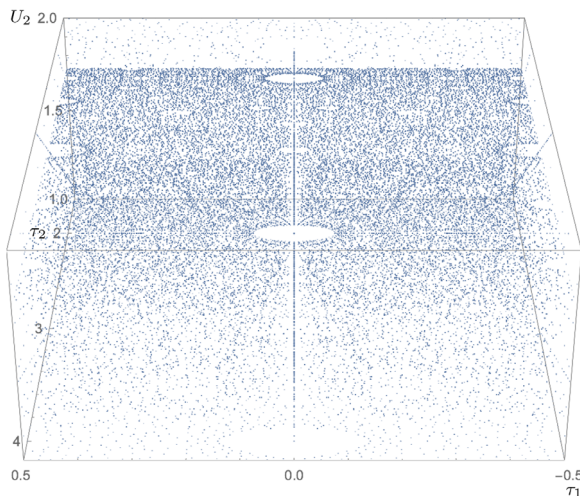
4.4. Summary

Let us summarize the results obtained in this section for the space of solutions of the combined axio-dilaton and complex-structure-moduli system with fluxes characterized by the setting described in section 4.1:

- As known before, for a fixed D3-brane tadpole contribution Q^0 the number of physically-distinct solutions to the F-term Equations (2.46) for the axio-dilaton and complex-structure moduli is finite. This is again due to the $SL(2, \mathbb{Z})$ dualities for the axio-dilaton and the complex-structure moduli.
- The values of the fixed moduli (mapped to their fundamental domains) are not distributed homogeneously in the space



(a) View along the line l_1 (orange) in figures 8.



(b) View along the line l_2 (red) in figures 8.

Figure 9. Section through the four-dimensional space of solutions with $U_1 = 0$ for the setting described in section 4.1. All solutions satisfy the bound $\frac{Q^0}{192} \leq 1000$ and have been mapped to the fundamental domains. The points of view are along the line l_1 (Figure 9a) and line l_2 (Figure 9b) in Figures 8, which show a void structure around l_1 and l_2 .

of solutions. As shown in Figures 9, the solutions are accumulated on submanifolds in the four-dimensional space with few points in between. We also find void structures in the space of solutions, which are however not spherical but take a cylindrical form in three-dimensional sections (cf. Figures 9).

- The imaginary parts of the axio-dilaton and the complex-structure moduli τ_2 and U_2 are bounded from above and below as shown in Equation (4.13). In our data we find however the stronger bound on the product $\tau_2 U_2 \leq \frac{3}{4} \frac{Q^0}{192}$, which implies that in the weak-coupling and large-complex-structure regime the tadpole contribution $\frac{Q^0}{192}$ has to be large. This is again in contrast to our arguments regarding the tadpole-cancellation condition on page 12 which requires $\frac{Q^0}{192}$ to be small, and illus-

trates the tension between the closed- and open-string sectors for obtaining reliable solutions.

- We have furthermore shown that the fraction of reliable flux solutions within all solutions for fixed tadpole $\frac{Q^0}{192}$ is only of orders $\mathcal{O}(10^{-3})$, which is a reduction as compared to the setting of section 3.

5. Moduli Stabilization III

We now generalize the setting from section 4 by including non-geometric Q -fluxes. The fluxes are restricted such that the complex-structure and Kähler moduli are fixed isotropically as $T_1 = T_2 = T_3 := T$ and $U^1 = U^2 = U^3 := U$, which reduces the system to the three complex moduli fields τ , U and T . Such vacua have previously been analyzed for instance in [23].

5.1. Setting

We specify the superpotential (2.42) by imposing the following restrictions on the R-R and NS-NS fluxes (2.34) and (2.35)

$$\begin{aligned} f^1 &= f^2 = f^3, & h^1 &= h^2 = h^3, \\ f_1 &= f_2 = f_3, & h_1 &= h_2 = h_3, \\ q^{01} &= q^{02} = q^{03}, \\ q_0^1 &= q_0^2 = q_0^3, \\ q^{11} &= q^{22} = q^{33}, & q^{12} &= q^{13} = q^{21} = q^{23} = q^{31} = q^{32} =: \tilde{q}^{11}, \\ q_1^1 &= q_2^2 = q_3^3, & q_1^2 &= q_1^3 = q_2^1 = q_2^3 = q_3^1 = q_3^2 =: \tilde{q}_1^1, \end{aligned} \quad (5.1)$$

which leaves four independent R-R F -flux components, four independent H -flux components and six independent Q -flux components. As discussed around Equation (2.37), these fluxes are subject to the quantization conditions

$$f^0, f^1, f_0, f_1, h^0, h^1, h_0, h_1, q^{01}, q^{11}, \tilde{q}^{11}, q_0^1, q_1^1, \tilde{q}_1^1 \in 8\mathbb{Z}. \quad (5.2)$$

Together with the Kähler potential (2.41), the F-term Equations (2.46) can then be determined explicitly. Since in the present situation the superpotential W depends on the Kähler moduli T_A , the condition $W = 0$ is in general not obtained and the resulting system of equations is more involved. However, provided that solutions to the F-term equations with non-vanishing imaginary parts exist, then for the fluxes (5.1) the moduli are stabilized isotropically

$$U^1 = U^2 = U^3 =: U, \quad T_1 = T_2 = T_3 =: T. \quad (5.3)$$

A necessary condition to achieve this stabilization is that $q_1^1 \neq \tilde{q}_1^1$ and $q^{11} \neq \tilde{q}^{11}$. The system of seven F-term equations for τ , U^i , T_A then reduces to the following three equations

$$\begin{aligned} 0 &= [f_0 - h_0 \bar{\tau} - q_0^1 3 T] + 3 U [f_1 - h_1 \bar{\tau} - (2 \tilde{q}_1^1 + q_1^1) T] \\ &\quad - (U)^3 [f^0 - h^0 \bar{\tau} - q^{01} 3 T] \\ &\quad + 3 (U)^2 [f^1 - h^1 \bar{\tau} - (2 \tilde{q}^{11} + q^{11}) T], \end{aligned} \quad (5.4a)$$

$$0 = [f_0 - h_0 \tau - q_0^1 (\bar{T} + 2T)] + 3U[f_1 - h_1 \tau - (2\bar{q}_1^1 + q_1^1) \frac{1}{3} (\bar{T} + 2T)] - (U)^3 [f^0 - h^0 \tau - q^{01} (\bar{T} + 2T)] + 3(U)^2 [f^1 - h^1 \tau - (2\bar{q}^{11} + q^{11}) \frac{1}{3} (\bar{T} + 2T)], \quad (5.4b)$$

$$0 = [f_0 - h_0 \tau - q_0^1 3T] + (\bar{U} + 2U)[f_1 - h_1 \tau - (2\bar{q}_1^1 + q_1^1)T] - \bar{U}(U)^2 [f^0 - h^0 \tau - q^{01} 3T] + (2\bar{U}U + (U)^2)[f^1 - h^1 \tau - (2\bar{q}^{11} + q^{11})T]. \quad (5.4c)$$

The R-R and NS-NS fluxes are furthermore subject to the Bianchi identities (2.38), and using the restrictions (5.1) we find for the tadpole contributions

$$\begin{aligned} Q^0 &= f_0 h^0 - f^0 h_0 + 3(f_1 h^1 - f^1 h_1), \\ Q^1 &= f_0 q^{01} - f^0 q_0^1 + 2(f_1 \bar{q}^{11} - f^1 \bar{q}_1^1) + f_1 q^{11} - f^1 q_1^1, \\ Q^{01} &= h_0 q^{01} - h^0 q_0^1 + 2(h_1 \bar{q}^{11} - h^1 \bar{q}_1^1) + h_1 q^{11} - h^1 q_1^1 \stackrel{!}{=} 0. \end{aligned} \quad (5.5)$$

Finally, as we discussed in section 2.4, the present setting is duality invariant under $SL(2, \mathbb{Z})$ transformations of the complex-structure modulus U whereas the $SL(2, \mathbb{Z})$ duality (2.56) of the axio-dilaton is broken to constant shifts (2.57) due to the non-vanishing Q -flux. Furthermore, T-duality (2.54) is in general broken because of the isotropic choice of fluxes in (5.1).

5.2. Infinite Number of Solutions for Fixed Q^A

In contrast to the settings of sections 3 and 4, for non-vanishing Q -flux the number of solutions for fixed tadpole contributions Q^A is infinite.^[23] This can be illustrated with the following example from [23]: the D7-brane tadpole contribution is fixed as $Q^1 = 0$ and the fluxes are chosen as follows

$$\begin{aligned} f^0 &= 0, & f^1 &= 0, \\ f_0 &= \frac{Q^0}{b}, & f_1 &= 0, \\ h^0 &= b, & h^1 &= b, \\ h_0 &= b, & h_1 &= -b, \\ q^{01} &= 0, & q^{11} &= -m, & \bar{q}^{11} &= 0, \\ q_0^1 &= -m - n, & q_1^1 &= n, & \bar{q}_1^1 &= m, \end{aligned} \quad (5.6)$$

where $m, n \in 8\mathbb{Z}$ and $b \in 8\mathbb{Z}$ is restricted such that $f_0 \in 8\mathbb{Z}$. To obtain non-trivial solutions we require $m, n, b \neq 0$, and the above choice of fluxes always satisfies the Bianchi identities (5.5). A solution to the equations of motion (5.4a) is given by

$$\tau = \frac{m^3 Q^0}{8b^2 n^3} (-4 \pm i), \quad U = \frac{m+n}{m} \pm \frac{n}{m} i, \quad T = \frac{m Q^0}{4b n^2} (2 \pm i), \quad (5.7)$$

where the sign takes the same value for all three moduli. In order for the imaginary parts to be positive we require that this sign is chosen appropriately and that $Q^0 > 0$ and $b n > 0$.

Note that (5.7) describes an infinite set of vacua since m, n are not bounded, which is in contrast to the situations studied in sections 3 and 4. However, in order to trust these solutions we have to require that $\text{Im } \tau, \text{Im } U, \text{Im } T > 1$ which translates into the conditions

$$1 < \left(\pm \frac{n}{m}\right)^3 < \frac{Q^0}{8b^2} \quad 1 < \pm \frac{n}{m} < \frac{Q^0}{4bn}. \quad (5.8)$$

For a fixed Q^0 there is only a finite number of choices for (m, n, b) which satisfy (5.8), and therefore the number of reliable solutions for the particular flux choice (5.6) is finite for fixed Q^0 . We remark however that duality transformations can change the form of (5.6), and therefore a similar analysis has to be performed for the transformed flux choices. We do not know whether this leads to a finite number of reliable flux solutions.

5.3. Space of Solutions

Since the number of physically-distinct solutions for fixed tadpole contributions Q^A is in general infinite, for the present setting we cannot construct a complete data set of flux vacua for fixed tadpole contribution. However, we can generate flux vacua using Monte-Carlo sampling.

Data Set

Our data set of flux vacua for the setting described in section 5.1 has been obtained in the following way:

- We restrict the contributions to the D3- and D7-brane tadpoles Q^0 and Q^1 shown in Equations (5.5) as

$$\left| \frac{Q^0}{64} \right| \leq 1000, \quad \left| \frac{Q^1}{64} \right| \leq 1000, \quad Q^{01} = 0. \quad (5.9)$$

Note that due to the flux-quantization condition (5.2) the Q^A are always a multiple of 64, and that Q^0 and Q^1 can be negative while still leading to positive imaginary parts for τ, U, T .

- The fluxes in (5.1) are chosen randomly with a uniform distribution. The restriction on the value of the fluxes reads

$$\left| \frac{\text{flux quantum}}{8} \right| \leq 100. \quad (5.10)$$

- We have generated $1.3 \cdot 10^7$ flux configurations for which 1) all moduli τ, U, T are fixed, 2) all imaginary parts of the moduli fields are strictly positive, and 3) the vacua are physically distinct (i.e. not related by $SL(2, \mathbb{Z})$ transformations of the complex-structure moduli nor by T -transformations of the axio-dilaton or Kähler moduli).
- For these flux contributions all moduli are fixed, however, not all of these extrema are stable. The number of vacua with all moduli fixed and without tachyonic or flat directions is $2.9 \cdot 10^6$.

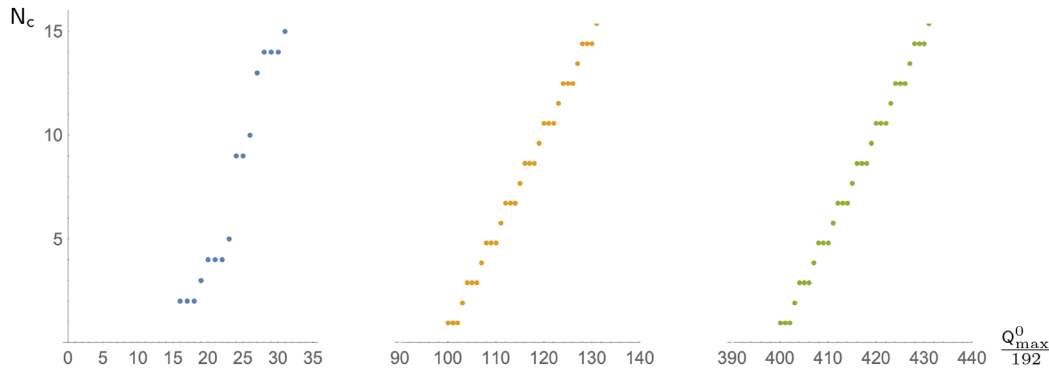


Figure 10. Number of solutions N_c as a function of $\frac{Q_{\max}^0}{192}$ (for the setting described in section 4.1) which satisfy $\tau_2, U_2 \geq c$ for $c = 2, 5, 10$ in colors blue, orange and green, respectively. Note that different ranges for $\frac{Q_{\max}^0}{192}$ on the horizontal axis.

Solutions at Small Coupling, Large Complex Structure and Large Volume

Since we do not have a complete set of solutions for fixed tadpole contributions Q^0 and Q^1 , the same analysis as for the previous cases cannot be performed. However, for our data set we have determined the number of solutions N_c for which $\tau_2 = \text{Im } \tau$, $U_2 = \text{Im } U$ and $T_2 = \text{Im } T$ satisfy

$$\tau_2, U_2, T_2 \geq c. \quad (5.11)$$

For sufficiently large c , this corresponds to the weak-coupling, large-complex-structure and large-volume regime. We furthermore denote by $|Q^A/64|_{\min}$ the lowest value of the expression $|Q^A/64| = \sqrt{(Q^0)^2 + 3(Q^1)^2}/64$ in the set of vacua determined by (5.11). For configurations which fix all moduli but may contain tachyonic directions we find:

c	N_c	N_c/N_0	$ Q^A/64 _{\min}$
0	$1.33 \cdot 10^7$	1	1
1	$5.97 \cdot 10^5$	$4.5 \cdot 10^{-2}$	16.7
2	$2.11 \cdot 10^4$	$1.6 \cdot 10^{-3}$	42.1
3	190	$1.4 \cdot 10^{-5}$	129.8
5	6	$4.5 \cdot 10^{-7}$	811.8

(5.12)

From here we see that vacua with large imaginary parts τ_2, U_2, T_2 are extremely rare but not excluded. For larger c – that is for more reliable solutions – the tadpole contributions have to be larger. These observations are in line with the results of the previous sections. For the stabilized vacua (without flat or tachyonic directions) we obtain a similar behaviour:

c	N_c	N_c/N_0	$ Q^A/64 _{\min}$
0	$2.94 \cdot 10^6$	1	1
1	$5.64 \cdot 10^5$	$1.9 \cdot 10^{-1}$	16.7
2	$2.03 \cdot 10^4$	$6.9 \cdot 10^{-3}$	42.1
3	163	$5.5 \cdot 10^{-5}$	129.8
5	1	$3.4 \cdot 10^{-7}$	1707.4

(5.13)

In **Table 1** we have collected some concrete examples for fully stabilized vacua with imaginary parts greater than one.

Distribution of Solutions in the Q^A -Plane

For moduli stabilization of the axio-dilaton and complex-structure moduli studied in sections 3 and 4 we observed that the tadpole-contribution Q^0 has to be positive in order to obtain physical solutions with positive imaginary parts τ_2 and U_2 . However, when including non-geometric fluxes we see that positive as well as negative values of Q^0 and Q^1 can result in positive imaginary parts τ_2, U_2 and T_2 .

Having a large data set available, we have analyzed the distributions of vacua over Q^0 and Q^1 . For the set of stable vacua without flat or tachyonic directions we obtain

Q^0	Q^1	fraction of all vacua
≤ 0	≤ 0	0.518765
≤ 0	> 0	0.155262
> 0	≤ 0	0.325822
> 0	> 0	0.000151

(5.14)

It is somewhat surprising that the fraction of vacua with tadpole contributions $Q^0 > 0$ and $Q^1 > 0$ is suppressed by three orders of magnitude compared to having at least one Q^A negative, but we have no explanation for that. For our data set of solutions which include potentially tachyonic directions no such difference is found

Q^0	Q^1	fraction of all vacua
≤ 0	≤ 0	0.360664
≤ 0	> 0	0.256953
> 0	≤ 0	0.254567
> 0	> 0	0.127816

(5.15)

We also note that both data sets do not contain any solution with $Q^0 = Q^1 = 0$.

Distribution of Solutions in Moduli Space

We have also analyzed the distribution of solutions to the F-term Equations (2.46) within the moduli space. Since the density of solutions is very small, we were not able to identify any patterns or structures.

Table 1. Examples for stable vacua (no tachyonic or flat directions) with $\tau_2, U_2, T_2 > 1$.

Data	Example 1	Example 2	Example 3	Example 4	Example 5	Example 6
f_0	−40	224	−336	−112	176	296
f_1	−88	24	96	104	24	−368
f^0	−56	8	32	40	48	8
f^1	0	0	24	0	24	−16
h_0	−88	−64	−16	−96	72	200
h_1	0	64	96	0	0	624
h^0	0	−16	−24	0	0	−192
h^1	0	0	−8	−8	0	−24
q^{01}	0	8	8	0	0	72
q^{11}	56	−104	112	24	−136	64
\bar{q}^{11}	−16	48	−64	−16	48	0
q_0^{-1}	72	64	80	48	−112	−192
q_1^{-1}	−64	8	96	−32	−40	488
\bar{q}_1^{-1}	32	−56	−64	16	24	−608
$Q^0/64$	−77	−48	−10	21	−54	−31
$Q^1/64$	30	17	−94	−43	66	−193
τ	$+0.45 + 19.3i$	$−0.02 + 4.39i$	$−0.40 + 3.42i$	$+0.47 + 8.25i$	$+0.32 + 12.1i$	$−0.48 + 5.15i$
U	$+0.00 + 3.53i$	$−0.33 + 3.52i$	$−0.10 + 3.13i$	$+0.47 + 3.04i$	$+0.10 + 3.13i$	$+0.32 + 3.14i$
T	$+0.00 + 7.48i$	$+0.20 + 3.03i$	$+0.30 + 4.07i$	$−4.47 + 8.49i$	$−0.48 + 3.10i$	$−0.26 + 4.57i$

5.4. Summary

We briefly summarize the main results obtained in this section for the combined moduli stabilization of the axio-dilaton, complex-structure moduli and Kähler moduli by the fluxes shown in Equation (5.1):

- For fixed D3- and D7-brane tadpole contributions Q^0 and Q^1 the number of physically-distinct vacua is in general infinite.^[23] We therefore were not able to generate a complete data set but used Monte-Carlo methods to randomly generate $1.3 \cdot 10^7$ solutions to the F-term equations which fix all moduli.
- We have shown that reliable solutions at weak string coupling, large complex structure and large volume are only a small fraction of all vacua. For instance, stable solutions with $\tau_2, U_2, T_2 \geq 5$ make only a fraction of $3.4 \cdot 10^{-7}$ of all solutions. Requiring the solutions to be more reliable requires the tadpole contributions Q^A to be larger, which is in tension with the tadpole-cancellation condition as discussed on page 12.
- In Table 1 we have shown some concrete examples of stable vacua with axio-dilaton, complex-structure moduli and Kähler moduli fixed at imaginary parts greater than one.
- Finally, we have pointed out that stable vacua with all tadpole contributions Q^0 and Q^1 positive are statistically disfavored. We do not have an explanation for this observation.

6. Discussion

In this work we have studied moduli stabilization with R-R and NS-NS fluxes in type IIB string theory for the example of the $T^6/\mathbb{Z}_2 \times \mathbb{Z}_2$ orientifold. We have analyzed the interplay between

moduli stabilization and tadpole cancellation, in particular, we have shown how properties of the vacua depend on the flux contribution to the tadpole-cancellation condition.

Summary of Results

More concretely, the axio-dilaton and complex-structure moduli are fixed by geometric fluxes while the Kähler moduli are fixed at tree-level using non-geometric Q -flux. In section 3 we have focussed on the axio-dilaton only and mainly ignored the complex-structure and Kähler moduli. In section 4 we included the complex-structure moduli, and in section 5 we studied moduli stabilization for all closed-string moduli. We analyzed the space of solutions to the F-term equations for these settings and found that it is not homogenous:

- For the axio-dilaton the space of solutions contains characteristic void structures (see Figure 2).^[16,20] The radius of these voids depends on the flux contribution Q^0 to the tadpole-cancellation condition, and for larger Q^0 the radii become smaller. When including the complex-structure moduli, we observe that vacua are accumulated on submanifolds within the space of solutions (see Figure 8). On these planes we again find void structures, which are connected by lines between different planes. We therefore find cylindrical voids in (three-dimensional sections of) this four-dimensional space of solutions.

Furthermore, in section 2.2 we have argued that the flux contribution to the tadpole-cancellation condition cannot be arbitrarily large. In particular, for many known examples this contribution

is small. We have then contrasted this observation with the requirement of having reliable solutions at weak string-coupling, large complex structure and large volume:

- We have seen that the fraction of vacua with small string coupling $\tau_2 \gg 1$, large complex structure $U_2 \gg 1$ and large volume $T_2 \gg 1$ is small. For instance, within the approach followed in this paper around 20% of the solutions satisfy $\tau_2 \geq 5$, around 0.4% of the solutions satisfy τ_2 , $U_2 \geq 5$, and a fraction of around 10^{-7} of the solutions satisfy τ_2 , U_2 , $T_2 \geq 5$. This suggests that for a large number of moduli, only a very small fraction of the solutions can be trusted (within the tree-level approach used in this work).
- We have also observed that in order to find vacua at weak string-coupling, large complex structure and large volume the flux contribution to the tadpole-cancellation condition has to be large. For instance, within the approach followed in this paper for $\tau_2 \geq 5$ one needs $Q^0 \geq 3840$, for τ_2 , $U_2 \geq 5$ one needs $Q^0 \geq 38208$, and for τ_2 , U_2 , $T_2 \geq 5$ we have indications that one needs $|Q^A| \gtrsim \mathcal{O}(10^5)$. This suggests that in order to stabilize a large number of moduli in a perturbatively-controlled regime a large flux contribution is needed. However, this conclusion is in stark contrast to the tadpole-cancellation condition which strongly disfavors large flux contributions.

To conclude, in order to stabilize moduli in a reliable way a large flux contribution is needed — which is however strongly restricted by the tadpole-cancellation condition. We therefore see that moduli stabilization and model building in string theory cannot be approached independently but have to be addressed simultaneously. This is a difficult task.

Limitations and Future Directions

We now comment on the limitations of the analysis performed in this paper and on future directions:

- Our conclusions in this work are based on the study of a single compactification space. We believe that the $\mathbb{T}^6/\mathbb{Z}_2 \times \mathbb{Z}_2$ orientifold captures main features of the problem, but these have to be confirmed by other examples. We are planning to address this point in the future.
- In this work we have stabilized moduli at tree-level. Corrections to the effective theory can usually be ignored in the weak-coupling, large-complex-structure and large-volume regime, however, many of the obtained solutions are not in this regime. We therefore should repeat our analysis and include various corrections from the start, which in turn will modify the space of solutions.
- We have found that only a small fraction of solutions stabilize moduli in a perturbatively-controlled regime. This observation has implications for the landscape of string vacua, in particular, it suggests that the landscape may be smaller than naively expected. It would be desirable to make this statement more precise.
- The $SL(2, \mathbb{Z})$ duality of the axio-dilaton was broken by non-geometric Q -fluxes. Including so-called P -fluxes will restore

this duality and may help in showing that the corresponding space of solutions is finite.

- The contribution of orientifold planes to the tadpole-cancellation condition could only be estimated based on known examples. It would be desirable to have a criterium which can put a bound on the orientifold contribution for a particular compactification space.

Appendix: Finite Number of Solutions for Setting II

In this appendix we follow the proof of [20,60], that for the setting of section 4.1 the number of physically-distinct solutions is finite for fixed Q^0 . The important property for showing this are the $SL(2, \mathbb{Z})$ dualities of the axio-dilaton and complex-structure moduli summarized in section 2.4. Splitting the moduli into real and imaginary parts as

$$\tau = \tau_1 + i\tau_2, \quad U = U_1 + iU_2, \quad (\text{A.1})$$

we recall that the two Equations (4.5) define an overdetermined cubic system for U and therefore do not allow for a closed-form solution in the generic case. We will now follow the lines of [20, 60] to demonstrate how a closed solution can still be obtained for the physically relevant cases.

In order for a physical solution to exist, both equations have to share a common root with non-vanishing imaginary part. Since all coefficients are real, there exists a second solution given by its complex conjugate and the two equations share a common quadratic factor. The two cubic polynomials (4.5) can then be factorized as

$$\begin{aligned} (rU + s)P(U) &= 0, \\ (uU + v)P(U) &= 0, \end{aligned} \quad (\text{A.2})$$

where $P(U)$ defines the common quadratic factor,

$$P(U) = l(U)^2 + mU + n, \quad (\text{A.3})$$

and the seven new variables $l, m, n, r, s, u, v \in \mathbb{Z}$ are defined by an overdetermined system of equations

$$\begin{aligned} rm + sl &= -3f^1, & rl &= f^0, \\ rn + sm &= -3f_1, & sn &= -f_0, \\ um + vl &= -3h^1, & ul &= h^0, \\ un + vm &= -3h_1, & vn &= -h_0. \end{aligned} \quad (\text{A.4})$$

The set of admissible septuples is furthermore restricted by requiring the flux quanta to satisfy the tadpole cancellation condition (4.7), which can be reformulated as

$$(rv - su)(m^2 - 4ln) = -3Q^0. \quad (\text{A.5})$$

As shown in [60], this condition can only be satisfied if Q^0 is a multiple of three, yielding an overall factor of 192 when taking into account the flux quantization conditions. Since the prefactors appearing in (A.2) are linear in U with real coefficients, the two solutions with non-vanishing imaginary part can be obtained by choosing U such that

$$P(U) = 0. \quad (\text{A.6})$$

Requiring furthermore the imaginary part of U to be positive, we arrive at the physical solutions

$$U = \frac{-m + \sqrt{m^2 - 4ln}}{2l} \quad \text{if } l > 0 \text{ and } n > 0,$$

$$U = \frac{-m - \sqrt{m^2 - 4ln}}{2l} \quad \text{if } l < 0 \text{ and } n < 0. \quad (\text{A.7})$$

The F-term Equation (4.6) is linear in τ and can be solved analytically, leading to the stabilized value

$$\tau = \frac{s(m + 2lU) + r[n + U(2m + 3lU)]}{v(m + 2lU) + u[n + U(2m + 3lU)]}. \quad (\text{A.8})$$

We will now proceed similarly to section 3.2 to show that using the dualities for the axio-dilaton and complex-structure moduli, for fixed Q^0 only a finite number of solutions can be found. Without loss of generality we focus on the case $l > 0$ and $n > 0$, but the situation $l < 0$ and $n < 0$ is completely analogous.

- As can be read-off from the first line in (A.7), the shift symmetry (2.49) of U gives rise to an equivalence

$$m \sim m + 2bl \quad b \in \mathbb{Z}. \quad (\text{A.9})$$

It therefore follows that all inequivalent values of m are contained in the range

$$m = -l, \dots, l-1. \quad (\text{A.10})$$

- Considering the boundary $U_2 = -\frac{1}{2}$, a minimal requirement for U to be located in the fundamental domain \mathcal{F}_U is given by $U_2 \geq \sqrt{3}/2$. This is equivalent to requiring

$$m^2 - 4ln \leq -3l^2. \quad (\text{A.11})$$

On the other hand, both of the factors on the left-hand side of the tadpole-cancellation condition (A.5) have to be integers, giving rise to a lower bound

$$m^2 - 4ln \geq -3Q^0. \quad (\text{A.12})$$

This restricts the inequivalent values of both l and n to finite ranges

$$1 \leq l \leq \sqrt{Q^0} \quad \frac{3l^2 + m^2}{4l} \leq n \leq \frac{3Q^0 + m^2}{4l}. \quad (\text{A.13})$$

- Employing the same arguments for the axio-dilaton, one finds an additional equivalence

$$s \sim s + bv \quad b \in \mathbb{Z} \quad (\text{A.14})$$

as well as upper bounds for u and v .

- The remaining degree of freedom r is fixed by the tadpole cancellation condition (A.5).

The above conditions leave only a finite number of inequivalent solutions for a fixed D3-tadpole contribution Q^0 .

Acknowledgements

The authors want to thank R. Blumenhagen, M. Haack, D. Klaewer, S. Krippendorff, C. Long, L. McAllister and L. Schlechter for very helpful discussions. EP thanks the Lorentz Institute for Theoretical Physics at the University in Leiden for its hospitality, and he thanks the organizers of the BIRS-CMO workshop “Geometrical Tools for String Cosmology” in Oaxaca where preliminary results of this work have first been presented.

Conflict of Interest

The authors have declared no conflict of interest.

Keywords

moduli stabilization, string theory

Received: July 12, 2019
Published online: August 9, 2019

- [1] R. Blumenhagen, B. K rs, D. L st, S. Stieberger, *Phys. Rept.* **2007**, 445, 1, hep-th/0610327.
- [2] D. S. Freed, E. Witten, *Asian J. Math.* **1999**, 3, 819, hep-th/9907189.
- [3] K. Dasgupta, G. Rajesh, S. Sethi, *JHEP* **1999**, 08, 023, hep-th/9908088.
- [4] T. R. Taylor, C. Vafa, *Phys. Lett.* **2000**, B474, 130, hep-th/9912152.
- [5] S. B. Giddings, S. Kachru, J. Polchinski, *Phys. Rev.* **2002**, D66, 106006, hep-th/0105097.
- [6] J.-P. Derendinger, C. Kounnas, P. M. Petropoulos, F. Zwirner, *Nucl. Phys.* **2005**, B715, 211, hep-th/0411276.
- [7] G. Villadoro, F. Zwirner, *JHEP* **2005**, 06, 047, hep-th/0503169.
- [8] O. DeWolfe, A. Giriyavets, S. Kachru, W. Taylor, *JHEP* **2005**, 07, 066, hep-th/0505160.
- [9] S. Kachru, R. Kallosh, A. D. Linde, S. P. Trivedi, *Phys. Rev.* **2003**, D68, 046005, hep-th/0301240.
- [10] V. Balasubramanian, P. Berglund, J. P. Conlon, F. Quevedo, *JHEP* **2005**, 03, 007, hep-th/0502058.
- [11] G. Obied, H. Ooguri, L. Spodyneiko, C. Vafa, “De Sitter Space and the Swampland,” 1806.08362.
- [12] R. Blumenhagen, S. Moster, E. Plauschinn, *JHEP* **2008**, 01, 058, 0711.3389.
- [13] S. Ashok, M. R. Douglas, *JHEP* **2004**, 01, 060, hep-th/0307049.
- [14] M. R. Douglas, *JHEP* **2003**, 05, 046, hep-th/0303194.
- [15] M. R. Douglas, B. Shiffman, S. Zelditch, *J. Diff. Geom.* **2006**, 72, 381, math/0406089.
- [16] F. Denef, M. R. Douglas, *JHEP* **2004**, 05, 072, hep-th/0404116.
- [17] A. Giriyavets, S. Kachru, P. K. Tripathy, *JHEP* **2004**, 08, 002, hep-th/0404243.
- [18] M. R. Douglas, *Comptes Rendus Physique* **2004**, 5, 965, hep-th/0409207.
- [19] J. P. Conlon, F. Quevedo, *JHEP* **2004**, 10, 039, hep-th/0409215.
- [20] O. DeWolfe, A. Giriyavets, S. Kachru, W. Taylor, *JHEP* **2005**, 02, 037, hep-th/0411061.
- [21] F. Denef, M. R. Douglas, *JHEP* **2005**, 03, 061, hep-th/0411183.
- [22] T. Eguchi, Y. Tachikawa, *JHEP* **2006**, 01, 100, hep-th/0510061.
- [23] J. Shelton, W. Taylor, B. Wecht, *JHEP* **2007**, 02, 095, hep-th/0607015.
- [24] D. Martinez-Pedraza, D. Mehta, M. Rummel, A. Westphal, *JHEP* **2013**, 06, 110, 1212.4530.
- [25] G. Dibitetto, A. Guarino, D. Roest, *JHEP* **2011**, 03, 137, 1102.0239.
- [26] B. S. Acharya, F. Denef, R. Valandro, *JHEP* **2005**, 06, 056, hep-th/0502060.

- [27] T. Watari, *JHEP* **2015**, 11, 065, 1506.08433.
- [28] M. Cirafici, *JHEP* **2016**, 03, 045, 1512.01170.
- [29] A. Cole, G. Shiu, *JHEP* **2019**, 03, 054, 1812.06960.
- [30] J. Halverson, C. Long, B. Sung, *JHEP* **2018**, 02, 113, 1710.09374.
- [31] I. Bena, E. Dudas, M. Graña, S. Lust, *Fortsch. Phys.* **2019**, 67, 1800100, 1809.06861.
- [32] J. Blaback, U. Danielsson, G. Dibitetto, "A new light on the darkest corner of the landscape," 1810.11365.
- [33] N. Cabo Bizet, C. Damian, O. Loaiza-Brito, D. M. Peña, "Leaving the Swamp: Non-geometric fluxes and the Distance Conjecture," 1904.11091.
- [34] T. W. Grimm, J. Louis, *Nucl. Phys.* **2004**, B699, 387, hep-th/0403067.
- [35] I. Benmachiche, T. W. Grimm, *Nucl. Phys.* **2006**, B748, 200, hep-th/0602241.
- [36] J. Shelton, W. Taylor, B. Wecht, *JHEP* **2005**, 10, 085, hep-th/0508133.
- [37] R. Blumenhagen, A. Font, E. Plauschinn, *JHEP* **2015**, 12, 122, 1507.08059.
- [38] M. Grana, *Phys. Rept.* **2006**, 423, 91, hep-th/0509003.
- [39] G. Villadoro, F. Zwirner, *JHEP* **2006**, 03, 087, hep-th/0602120.
- [40] P. Betzler, E. Plauschinn, *Nucl. Phys.* **2018**, B933, 384, 1712.08382.
- [41] E. Plauschinn, *Phys. Rept.* **2019**, 798, 1, 1811.11203.
- [42] E. Kiritsis, *String theory in a nutshell*. Princeton University Press **2007**.
- [43] R. Blumenhagen, E. Plauschinn, *Lect. Notes Phys.* **2009**, 779, 1.
- [44] A. Sagnotti, *Phys. Lett.* **1992**, B294, 196, hep-th/9210127.
- [45] R. Minasian, G. W. Moore, *JHEP* **1997**, 11, 002, hep-th/9710230.
- [46] P. S. Aspinwall, "D-branes on Calabi-Yau manifolds," in *Progress in string theory*. Proceedings, Summer School, TASI 2003, Boulder, USA, June 2–27, 2003, pp. 1–152, **2004**. hep-th/0403166.
- [47] R. Blumenhagen, A. Font, M. Fuchs, D. Herschmann, E. Plauschinn, Y. Sekiguchi, F. Wolf, *Nucl. Phys.* **2015**, B897, 500, 1503.07634.
- [48] E. Plauschinn, *JHEP* **2009**, 05, 062, 0811.2804.
- [49] D. Lust, S. Reffert, E. Scheidegger, S. Stieberger, *Adv. Theor. Math. Phys.* **2008**, 12, 67, hep-th/0609014.
- [50] R. Blumenhagen, V. Braun, T. W. Grimm, T. Weigand, *Nucl. Phys.* **2009**, B815, 1, 0811.2936.
- [51] P. Candelas, E. Peralvalov, G. Rajesh, *Nucl. Phys.* **1997**, B507, 445, hep-th/9704097.
- [52] M. Lynker, R. Schimmrigk, A. Wisskirchen, *Nucl. Phys.* **1999**, B550, 123, hep-th/9812195.
- [53] W. Taylor, Y.-N. Wang, *JHEP* **2015**, 12, 164, 1511.03209.
- [54] D. Junghans, *Backreaction of Localised Sources in String Compactifications*. PhD thesis, Leibniz U., Hannover, **2013**. 1309.5990.
- [55] A. Font, L. E. Ibanez, F. Quevedo, *Phys. Lett.* **1989**, B217, 272.
- [56] M. Berkooz, R. G. Leigh, *Nucl. Phys.* **1997**, B483, 187, hep-th/9605049.
- [57] I. Antoniadis, C. Bachas, C. Fabre, H. Partouche, T. R. Taylor, *Nucl. Phys.* **1997**, B489, 160, hep-th/9608012.
- [58] D. Lust, S. Reffert, W. Schulgin, S. Stieberger, *Nucl. Phys.* **2007**, B766, 68, hep-th/0506090.
- [59] A. R. Frey, J. Polchinski, *Phys. Rev.* **2002**, D65, 126009, hep-th/0201029.
- [60] S. Kachru, M. B. Schulz, S. Trivedi, *JHEP* **2003**, 10, 007, hep-th/0201028.
- [61] R. Blumenhagen, D. Lust, T. R. Taylor, *Nucl. Phys.* **2003**, B663, 319, hep-th/0303016.
- [62] J. F. G. Cascales, A. M. Uranga, *JHEP* **2003**, 05, 011, hep-th/0303024.
- [63] C. Vafa, *Nucl. Phys.* **1986**, B273, 592.
- [64] T. H. Buscher, *Phys. Lett.* **1987**, B194, 59.
- [65] T. H. Buscher, *Phys. Lett.* **1988**, B201, 466.
- [66] E. Plauschinn, *Nucl. Phys.* **2015**, B893, 257, 1408.1715.
- [67] S. F. Hassan, *Nucl. Phys.* **2000**, B568, 145, hep-th/9907152.
- [68] G. Aldazabal, P. G. Camara, A. Font, L. E. Ibanez, *JHEP* **2006**, 05, 070, hep-th/0602089.
- [69] G. Aldazabal, P. G. Camara, J. A. Rosabal, *Nucl. Phys.* **2009**, B814, 21, 0811.2900.
- [70] A. Guarino, G. J. Weatherill, *JHEP* **2009**, 02, 042, 0811.2190.
- [71] A. Chatzistavrakidis, F. F. Gautason, G. Moutsopoulos, M. Zagermann, *Phys. Rev.* **2014**, D89, 066004, 1309.2653.
- [72] Y. Sakatani, *JHEP* **2015**, 03, 135, 1412.8769.
- [73] E. A. Bergshoeff, V. A. Penas, F. Riccioni, S. Risoli, *JHEP* **2015**, 11, 020, 1508.00780.
- [74] P. Shukla, *JHEP* **2015**, 11, 075, 1505.00544.
- [75] D. M. Lombardo, F. Riccioni, S. Risoli, *JHEP* **2016**, 12, 114, 1610.07975.